NAVAL POSTGRADUATE SCHOOL
Monterey, California

THESIS

NOGAPS VERIFICATION USING SPECTRAL COMPONENTS

by

Peter A. Morse

March 1983

Thesis Advisor: C. H. Wash

Approved for public release; distribution unlimited.

T208048

LIBRARY, NAVAL POSTGRADUATE SCHOOL
MONTEREY, CA 93940

REPORT DOCUMENTATION PAGE

READ INSTRUCTIONS
BEFORE COMPLETING FORM

1. REPORT NUMBER	2. GOVT ACCESSION NO.	3. RECIPIENT'S CATALOG NUMBER
4. TITLE (and Subtitle) NOGAPS Verification Using Spectral Components		5. TYPE OF REPORT & PERIOD COVERED Master's Thesis; March 1983
		6. PERFORMING ORG. REPORT NUMBER
7. AUTHOR(s) Peter A. Morse		8. CONTRACT OR GRANT NUMBER(s)
9. PERFORMING ORGANIZATION NAME AND ADDRESS Naval Postgraduate School Monterey, California 93940		10. PROGRAM ELEMENT, PROJECT, TASK AREA & WORK UNIT NUMBERS
11. CONTROLLING OFFICE NAME AND ADDRESS Naval Postgraduate School Monterey, California 93940		12. REPORT DATE March 1983
		13. NUMBER OF PAGES 71
14. MONITORING AGENCY NAME & ADDRESS(if different from Controlling Office)		15. SECURITY CLASS. (of this report) Unclassified
		15a. DECLASSIFICATION/DOWNGRADING SCHEDULE

16. DISTRIBUTION STATEMENT (of this Report)

Approved for public release; distribution unlimited.

17. DISTRIBUTION STATEMENT (of the abstract entered in Block 20, if different from Report)

18. SUPPLEMENTARY NOTES

19. KEY WORDS (Continue on reverse side if necessary and identify by block number)

Numerical Weather Prediction
Naval Operational Global Atmospheric Prediction System
Planetary Waves
Spectral Decomposition

20. ABSTRACT (Continue on reverse side if necessary and identify by block number)

In this study one three-day and two five-day Numerical Operational Global Atmospheric Prediction System (NOGAPS) 500mb forecasts were spectrally verified. The wavenumber components of the observed and forecast waves were grouped into planetary (wavenumbers 1-3), long (wavenumbers 5-7) and medium (wavenumbers 8-12) wavenumbers for verification. The observed and forecast trough-ridge (Hovmoller) diagrams of longitude versus time for each group were analyzed for each case.

In all three cases the most serious errors occurred in the planetary waves where the model often forecast erroneously large of small amplitudes. The long waves were the most accurately forecast group both in amplitude and phase speed. The medium wave amplitudes were forecast too weak and phase speeds were consistantly too fast for this group.

Approved for public release; distribution unlimited

NOGAPS Verification Using Spectral Components

by

Peter A. Morse
Captain, United States Air Force
B.S., North Carolina State University, 1976

Submitted in partial fulfillment of the
requirements for the degree of

MASTER OF SCIENCE IN METEOROLOGY

from the

NAVAL POSTGRADUATE SCHOOL
March 1983

Thesis
M83975
c.1

ABSTRACT

In this study one three-day and two five-day Numerical Operational Global Atmospheric Prediction System (NOGAPS) 500mb forecasts were spectrally verified. The wavenumber components of the observed and forecast waves were grouped into planetary (wavenumbers 1-3), long (wavenumbers 5-7) and medium (wavenumbers 8-12) wavenumbers for verification. The observed and forecast trough-ridge (Hovmoller) diagrams of longitude versus time for each group were analysed for each case.

In all three cases the most serious errors occurred in the planetary waves where the model often forecast erroneously large or small amplitudes. The long waves were the most accurately forecast group both in amplitude and phase speed. The medium wave amplitudes were forecast too weak and phase speeds were consistantly too fast for this group.

TABLE OF CONTENTS

I. INTRODUCTION 10

II. NOGAPS SUMMARY 14

III. SPECTRAL DECOMPOSITION ROUTINE 20

IV. SPECTRAL VERIFICATION CASE STUDIES 29

V. CONCLUSIONS AND SUGGESTIONS FOR FUTURE RESEARCH . . 64

LIST OF REFERENCES 68

INITIAL DISTRIBUTION LIST 70

LIST OF TABLES

TABLE I. The numerical results of the spectral decomposition. 23

LIST OF FIGURES

Figure 1. The Vertical Differencing of the NOGAPS Model 17

Figure 2. The Height contours of the 500mb Surface at 00Z 18 Feb. 21

Figure 3. The Height of the 500mb Surface Along 42N at 00Z 18 Feb. 21

Figure 4. The Relative Amplitudes of the Wavenumber 1-28 Components 24

Figure 5. The Height of the 500mb Surface and Wavenumber Components 24

Figure 6. Hovmoller Diagrams of the Wavenumber 3 Component 27

Figure 7. 500mb Heights and Wavenumber Components for 00Z 21 Feb. 31

Figure 8. Planetary Wave Hovmoller Diagrams for 18-21 Feb. 33

Figure 9. Wavenumber 1 and 3 Components for Case 1. . . 35

Figure 10. Long Wave Hovmoller Diagrams for 18-21 Feb. . 37

Figure 11. Medium Wave Hovmoller Diagrams for 18-21 Feb. 39

Figure 12. 500mb Heights and Wavenumber Components for 06 Oct. 41

Figure 13. Same as Fig.7 except for 09 Oct. 43

Figure 14. Same as Fig.7 except for 11 Oct. 45

Figure 15. Same as Fig. 8 except for 06-11 Oct. 46

Figure 16. Wavenumber 2, 3 and 5 Components for Case 2. 48

Figure 17. Same as Fig. 10 except for 06-11 Oct. 50

Figure 18. Same as Fig. 11 except for 06-11 Oct. 51

Figure 19. Same as Fig. 12 except for 22 Oct 54

Figure 20. Same as Fig. 7 except for 25 Oct 55

Figure 21. Same as Fig. 7 except for 27 Oct 57

Figure 22. Same as Fig. 8 except for 22-27 Oct 59

Figure 23. Wavenumber 3 component for Case 3. 60

Figure 24. Same as Fig. 10 except for 22-27 Oct 61

Figure 25. Same as Fig. 11 except for 22-27 Oct 62

ACKNOWLEDGEMENT

I would like to thank Dr. Carlyle H. Wash for his guidance during the preparation, development and writing of this thesis. His infectious enthusiasm and tireless efforts are directly responsible for its timely completion. I would like to thank Dr. R. T. Williams for his aid and assistance in employing his spectral decomposition routine and his editorial recommendations as second reader. I would like to thank Research Associate, Dr. James Boyle, who made FNOC data available to me, and Mr. David Ebel, who helped me process the data into a useable format, for freely contributing portions of their valuable time on short notice. I would like to thank Capt. Alan F. Shaffer, who said I would never make it, for his inspiration. And finally I would like to thank my wife, Suchada, for her pleasant company on the long, long nights in the W. R. Church Computer Center.

I. INTRODUCTION

Accurate and reliable numerical weather prediction is a major goal for civilian and military atmospheric studies. Verification studies are an important aspect of numerical model development as they isolate model strengths and weaknesses and identify errors which must be eliminated to extend the present limits of forecast skill.

This thesis will investigate the Naval Operational Global Atmospheric Prediction System (NOGAPS) model's ability to forecast the position and movement of 500mb waves in the mid latitudes of the Northern Hemisphere. NOGAPS, which became operational in September, 1982 at the Fleet Numerical Oceanography Center (FNOC) has been a project of the Naval Environmental Prediction Research Facility (NEPRF) since 1976. The long term goal of NOGAPS is to achieve a medium range (7-10 days) numerical forecast capability for the U.S. Navy (Rosmond,1981). Verification of NOGAPS is very important at this stage due to the research type background of the model. The NOGAPS forecast model is a modified form of the UCLA general circulation model. Consequently, it has not had the benefit of many prior intensive verification studies as have most second and third generation operational models.

Recent studies have raised serious questions concerning the relative accuracy of the planetary-scale (zonal wavenumbers 1-2) wave motion forecasts at 500mb produced by numerical weather prediction models. Lambert and Merilees (1978) concluded the planetary-scale motion predictions of a spectral numerical model were poorer with respect to persistence than long (wavenumbers 3-5) or medium-scale (wavenumbers 6-10) motions. Miyakoda et al. (1972) examined the GFDL model performance over a series of winter forecasts and found similar error characteristics in the planetary-scale forecasts. This study will verify NOGAPS planetary wave forecasts and other wave regimes, large and medium-scale.

500mb data from both the forecast and the analysis are spectrally decomposed into its basic components of amplitude and phase then organized into planetary, long and medium-scale waves for separate analysis of their atmospheric behavioral characteristics. If one assumes spatial coupling (the interacting of different scales), then model weaknesses in forecasting 'long' wave motion will be reflected in the accuracy of 'short' wave motion forecasts. The purpose of this study is to perform a thorough analysis of the forecasts of each wave grouping. Somerville (1980) examined the

planetary-scale wave forecasts of a primitive equation numerical model in both a global and hemispheric configuration. He concluded that the global version was markedly more skillful than the hemispheric version especially in the latter part of the five-day forecast period. While the present study will consider only a global version of NOGAPS the results will lend themselves to an application of Somerville's work to NOGAPS.

Errors in phase speeds, amplitudes, development of baroclinic systems, damping of smaller scale features and planetary wave structure become clearer when the forecasted variables are analyzed over time via a Hovmoller or trough-ridge plot. Baumhefner and Downey (1978) utilized this technique to intercompare the forecasting skills of three numerical weather prediction models. They constructed longitude-time plots along a fixed latitude to better understand the time evolution of the forecast fields. Forecasts which originally appeared quite good were revealed to have amplification errors in many of the transient systems. A spectral breakdown of the Hovmoller plot in planetary (wavenumbers 1-3), large (wavenumbers 5-7) and medium scale-waves (wavenumbers 8-12) were utilized in their study.

One has only to consider the complexity of a typical 500mb wave pattern to appreciate the benefits of this approach.

The specific objectives of this thesis are:

(1) Development of a spectral verification program using wavenumber grouping and Hovmoller plots for tropospheric height data,

(2) Application of the program to interesting NOGAPS forecast situations at 500mb,

(3) Use of wavenumber analysis to verify NOGAPS forecasts of planetary, long and medium-scale waves.

Chapter 2 reviews the main features of the NOGAPS model. The pattern decomposition program is described and demonstrated in chapter 3. Chapter 4 presents the basic characteristics of the case study periods and their subsequent atmospheric behavior. Finally, chapter 5 summarizes the results of the forecast comparison and makes suggestions for further research.

II. NOGAPS SUMMARY

The Naval Operational Global Atmospheric Prediction System (NOGAPS) was developed by the Naval Environmental Prediction Research Facility (NEPRF) to be run at the Fleet Numerical Oceanography Center (FNOC). The objectives of the NOGAPS project are to improve tropical and Southern Hemispheric forecasting and achieve mid-range (5 - 10 days) global numerical forecast capability to support U.S. Naval operations (Rosmond,1981).

The objective analysis method used by NOGAPS is a variation of the successive corrections technique (Barnes,1964) which discriminates among observing systems according to their accuracy. While the final analysis is not as sophisticated as the optimal interpolation method it requires far less computer resources.

Global mass and wind fields are analyzed independently with optional data bogusing. Data rejection criteria are intentionally loose since the initialization scheme (Barker,1981) removes the gravity waves excited by bad data. This technique prevents inadvertent rejection of the good data associated with rapidly developing systems.

A calculus of variation method combines the results of the wind and mass analyses. The hydrostatic equation permits substitution of temperature for geopotential which gives the forecast model three dimensionality. The form of NOGAPS initialization used in our study produces balanced geopotentials (temperatures) and non-divergent winds which are interpolated directly to the model's sigma coordinate system. The method which became operational in December, 1982, defines geopotential and wind as objective analyses correction fields. The resulting balanced corrections are interpolated to the sigma surfaces, as in the first method, and added to the first guess forecast. This method preserves the model-generated divergence and minimizes the vertical interpolation error.

The first guess forecast of specific humidity and the prognostic planetary boundary layer (PBL) variables are used as initial values for the subsequent forecast cycle. The six-hour update cycle is preferred over the twelve-hour configuration since less time interpolation of asynoptic data is required. However, the shorter cycle is more subject to initialization shock and relies heavily on the initialization technique to control the noise. Failure to do so may

result in subsequent first guess errors sufficiently large to cause rejection of good observational data.

The NOGAPS model is a modified version of the UCLA general circulation model (GCM) described by Arakawa and Lamb (1977). The 2.4 by 3.0 degree horizontal grid uses scheme C staggering of the variables and conserves energy and enstrophy when the flow is nondivergent. All dependent variables except vertical velocity are defined in the middle of each of the six vertical sigma levels (Fig. 1).

Moisture, moist static energy and momentum are assumed to be well-mixed in the PBL. The equations governing the diabatic processes are based on the method of Deardorff (1972). These equations represent the conservation of mass in the PBL, temperature and specific humidity inversion strength and the jump in momentum across the inversion. A special feature of the model is the variable depth of the PBL in the lowest layer which has a capping inversion of a porous material surface. This allows entrained mass to deepen the PBL and removed mass (by cumulus mass flux) to decrease the PBL. The fluxes at the top of the PBL are not a constant fraction of the surface fluxes but rather a function of the entrainment. Dissipating stratus causes a

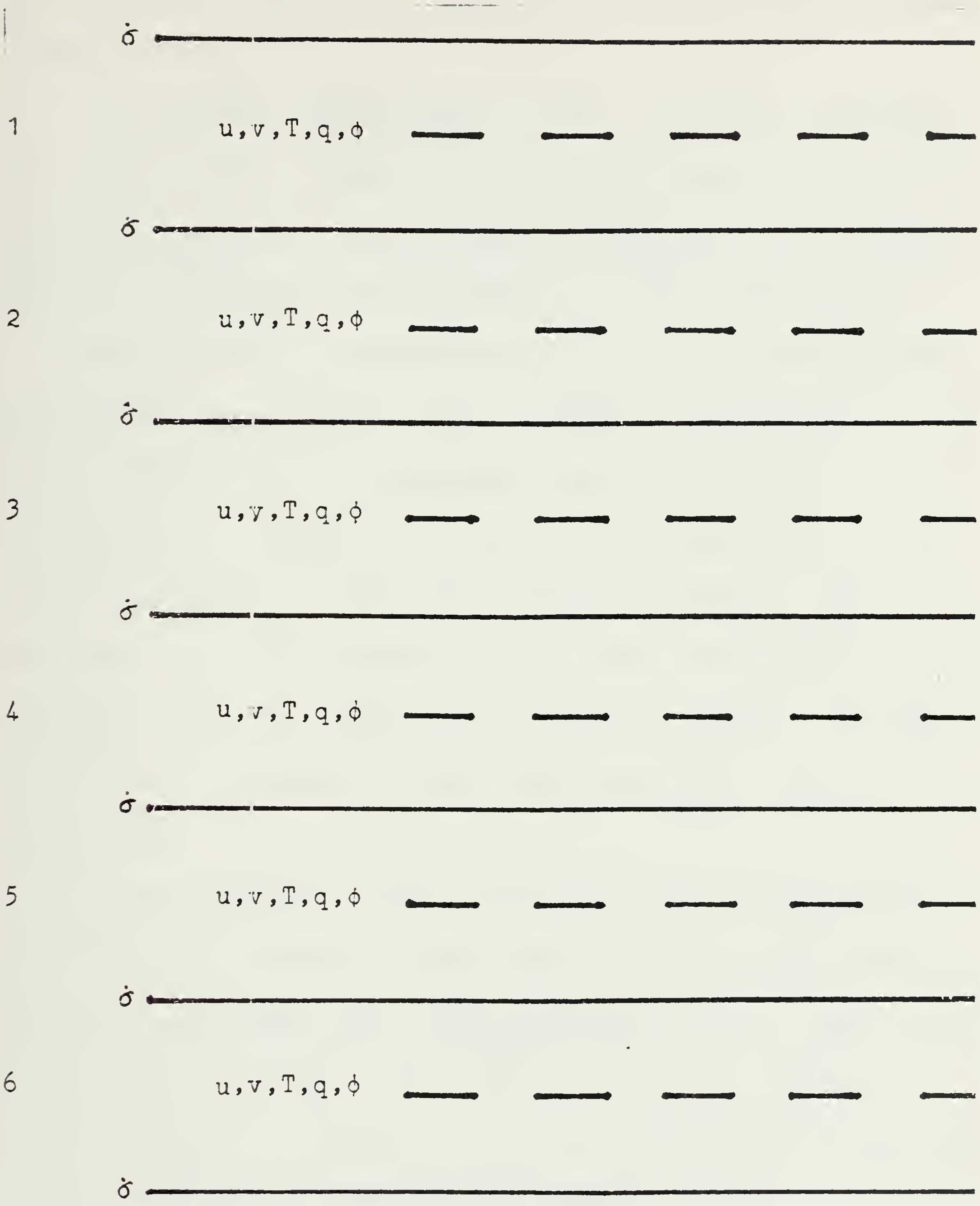

Figure 1. The Vertical Differencing of the NOGAPS Model

particularly large flux across the inversion for stratus capped PBL's.

A significant modification to the GCM is the constrainment of the PBL to remain in the bottom sigma layer. This eliminates serious computational problems yet has not created any noticeable adverse effects on model forecasts.

NOGAPS uses the Arakawa-Schubert (1974) cumulus parameterization described by Lord (1978). Environmental air below the cloud top is entrained while air at the cloud top is detrained. Arakawa noted that large scale forcing generates conditional stability whereas cumulus convection destroys it. This concept, called 'quasi-equilibrium', was combined with the 'cloud work' concept (Arakawa and Schubert, 1974) to produce a cloud base mass flux unique to each cloud type.

The GCM radiation parameterization requires only fifteen percent of the model's running time. The radiation transfer equation (Katayama, 1974 and Schlesinger, 1976) uses bulk transmission functions for discrete pressure layers. Net radiative flux at ground level is a function of incoming solar and longwave radiation and surface albedo.

NOGAPS is run on the CYBER 205 which has high speed scalar and vector pipeline processors. Presently, the forecast model has a wall clock execution time of thirty minutes per forecast day on a 2.4 X 3.0 degree grid. Any significant increase in the model's performance would require redesigning the diabatic processes to include more vectorization for the entire model.

III. SPECTRAL DECOMPOSITION ROUTINE

The complex appearance of a typical 500 mb height wave pattern often conceals the sources of forecast error. The pattern's complexity is due to the superposition of planetary, long, medium and synoptic waves. Every pattern, regardless of its intricacy, can be represented as the sum of a series of pure harmonic waves. A spectral decomposition routine will resolve a complex wave into its components, that is, the amplitude and phase angle of each wave number 1, 2, 3, etc. The spectral analysis used in this study was developed at the Naval Postgraduate School by Prof. R. T. Williams.

The 500 mb wave pattern along 42N (Fig. 2) for 18 February will be spectrally decomposed to illustrate the technique.

To facilitate this illustration and the foregoing sequence of illustrations, Fig. 3 has an abcissa/ordinate scale ratio of 25000km/60Cm or approximately 42000 to 1.

Note the negative longitudes are west and the positive longitudes are east. A careful examination of the heights

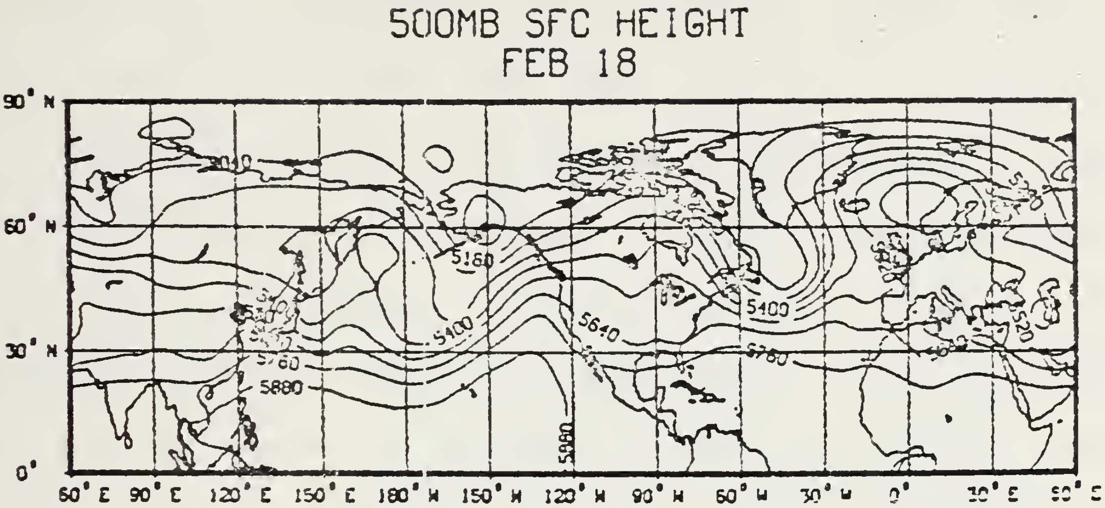

Figure 2. The Height contours of the 500mb Surface at 00Z 18 Feb. Contour Intervals are 120 Meters.

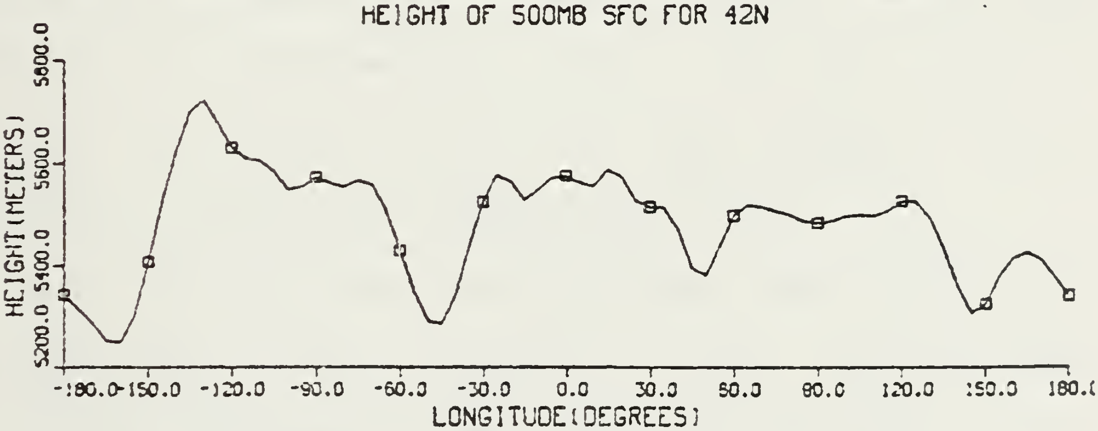

Figure 3. The Height of the 500mb Surface Along 42N at 00Z 18 Feb. The Negative and Positive Longitudes are West and East Respectively of the Greenwich Meridian. Boxes Appear at 30 Degree Intervals.

along 42N suggest a relatively significant amplitude of wavenumber 3 as evidenced by the prominent ridge locations in the vicinity of 120W, 0 and 90E. Also the preponderance of ridges and troughs in the 4000km (50-60 degrees) range are the signatures of wavenumbers 6 and 7. Since a minimum of six points is required to adequately resolve a wave, the maximum wavenumber accurately resolveable with a 72-point series (five degrees of longitude) is 12. A horizontal resolution of three degrees of longitude can accurately depict wavenumbers up to 20. Amplitude estimates are difficult and finer resolution would be speculative at best.

The numerical results of the decomposition routine are presented in Table 1 (although only wavenumbers 1 - 20 can be accurately resolved, the tables and figures in this study will represent wavenumbers 1 - 28). The phase angle and amplitude (in meters about the mean height) of the wavenumber 1 through 28 components are shown.

First the mean height was calculated, then the amplitude and phase angle of each wavenumber 1 - 28. The amplitudes are given as difference values about the mean height and the phase angles are in reference to the center of the longitudinal domain (0 degrees).

TABLE I

The numerical results of the spectral decomposition.

Spectral decomposition of 500mb wave at 42N. Amplitudes are in meters and the phases are in degrees.

ARITHMETIC MEAN	WAVE NUM	AMPLITUDE	PHASE
5485.91	1	52.04	-88.94
	2	66.67	27.38
	3	92.17	-157.89
	4	24.91	88.19
	5	26.40	126.31
	6	46.92	-41.79
	7	57.17	129.36
	8	13.86	134.82
	9	13.63	-0.63
	10	10.19	-115.47
	11	21.45	101.96
	12	10.36	135.11
	13	4.26	-41.04
	14	1.20	142.10
	15	6.06	111.40
	16	4.96	125.36
	17	9.54	77.27
	18	4.70	1.36
	19	4.54	64.28
	20	2.91	-52.99
	21	1.13	-96.49
	22	1.56	27.35
	23	0.46	-14.74
	24	1.30	-146.30
	25	0.42	-114.46
	26	1.17	136.61
	27	1.30	41.12
	28	0.65	-28.40

A graph of wave number versus amplitude (Fig. 4) further clarifies the high relative amplitudes of wavenumbers 3, 6 and 7 proposed by our initial visual analysis. The comparative importance of wavenumber 11 is also apparent.

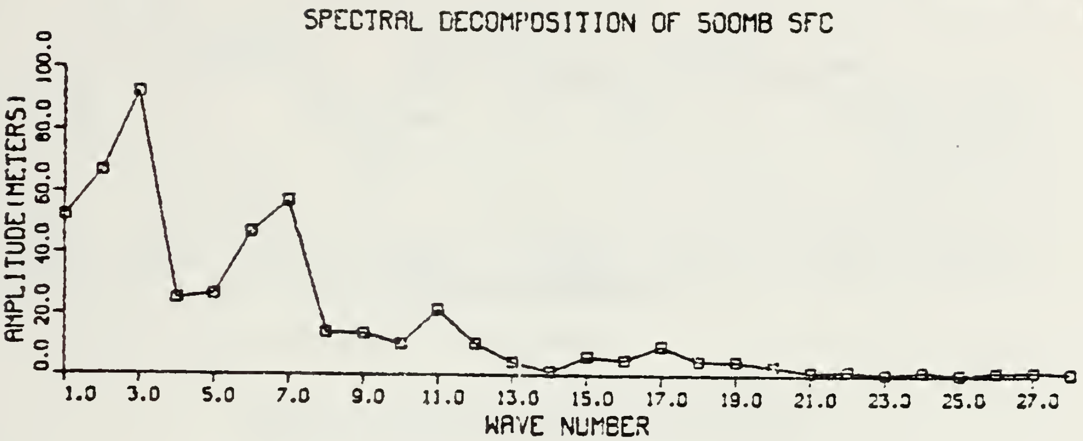

Figure 4. The Relative Amplitudes of the Wavenumber 1-28 Components of the 500mb Surface Along 42N at 00Z 18 Feb. Boxes Appear for each Wavenumber 1-28.

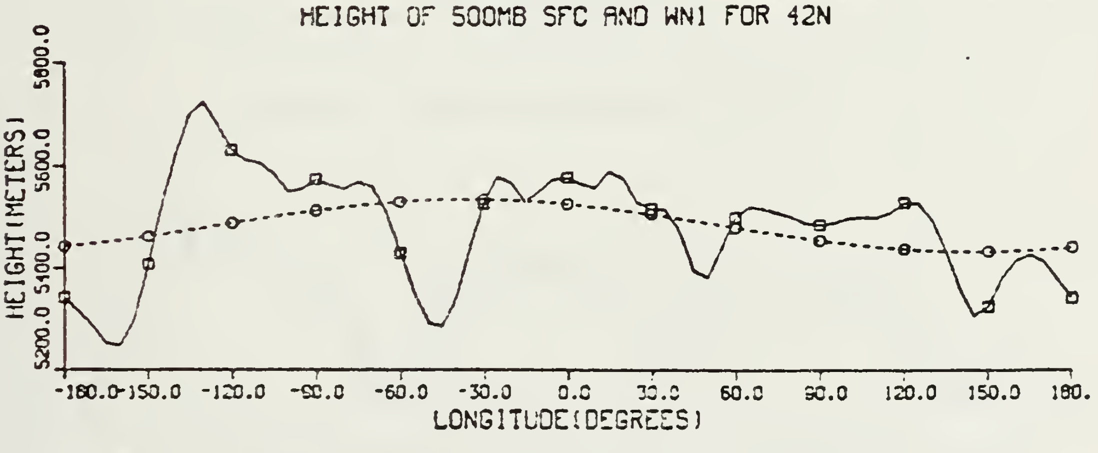

Figure 5. The Height of the 500mb Surface and Wavenumber Components Along 42N at 00Z on 18 Feb. The Negative and Positive Longitudes are West and East Respectively of the Greenwich Meridian. Boxes are Positioned at 30 Degree Intervals. a) Wavenumber 1 Component.

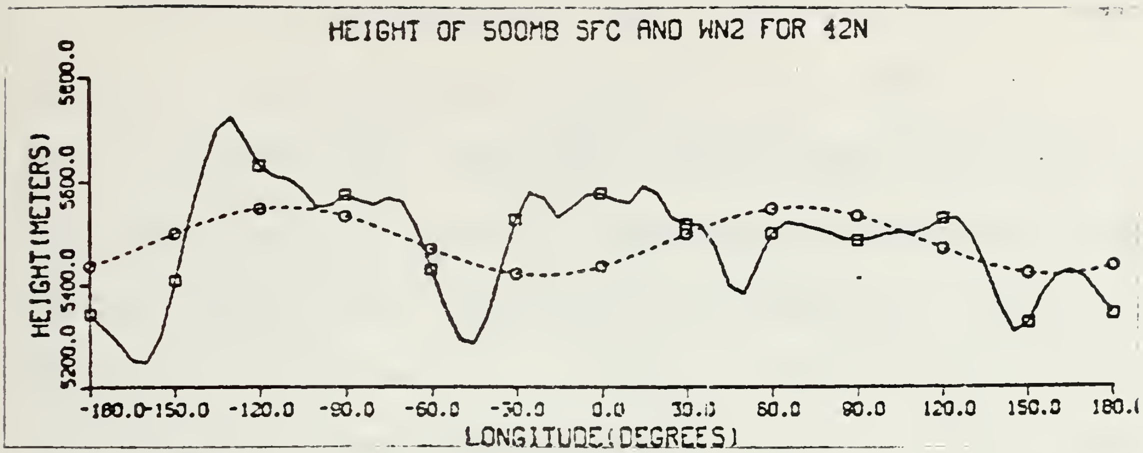

5b) Wavenumber 2 component

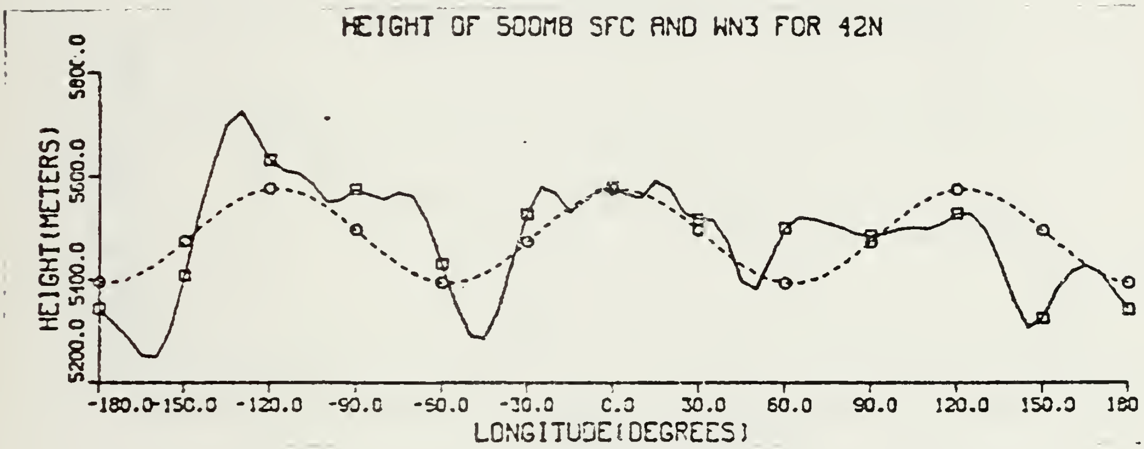

5c) Wavenumber 3 component

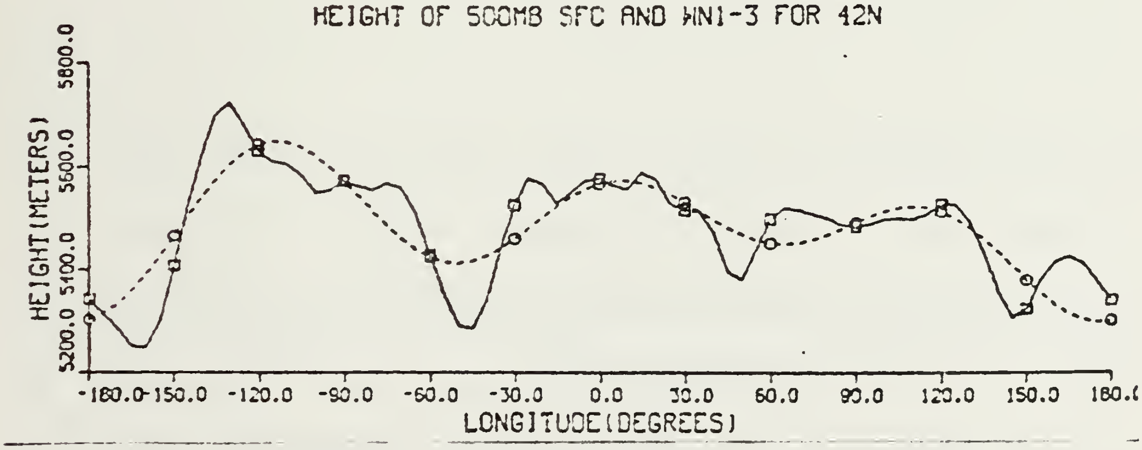

5d) Summation of wavenumber 1-3 components

The series of graphs in Figs. 5a-e elucidate the significance of the planetary component of the 500mb wave. All of these figures graph the height versus the longitude of the original wave (solid line) with various wavenumber combinations (dashed line) superposed for comparison. Figs. 5a, b and c chart wavenumbers 1, 2 and 3 respectively, while d is the summation of wavenumbers 1, 2 and 3.

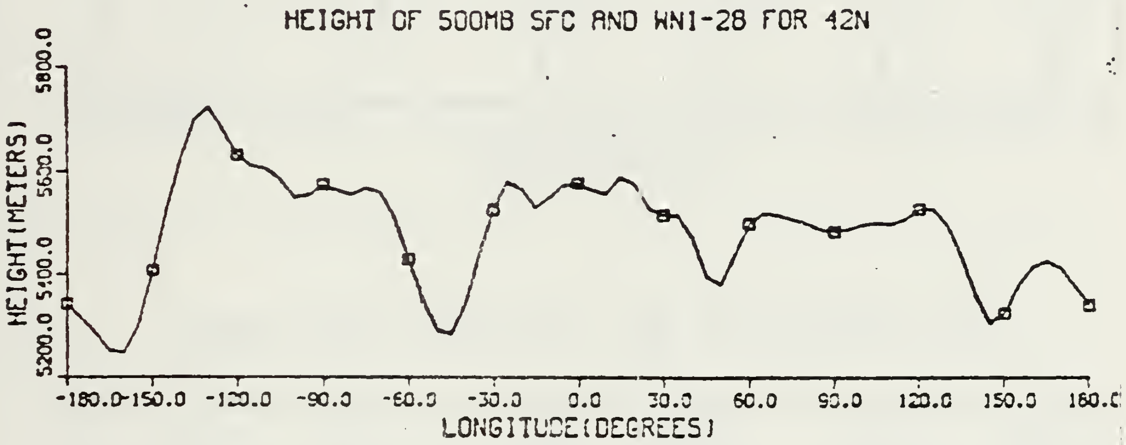

5e) Summation of wavenumber 1-28 components

Note how these three waves begin to resemble the original pattern. It is important to realize the summation of the full series of harmonic waves would reconstitute the 500 mb wave excepting any high frequency variations (greater than wavenumber 28) present in the original wave. Fig. 5e

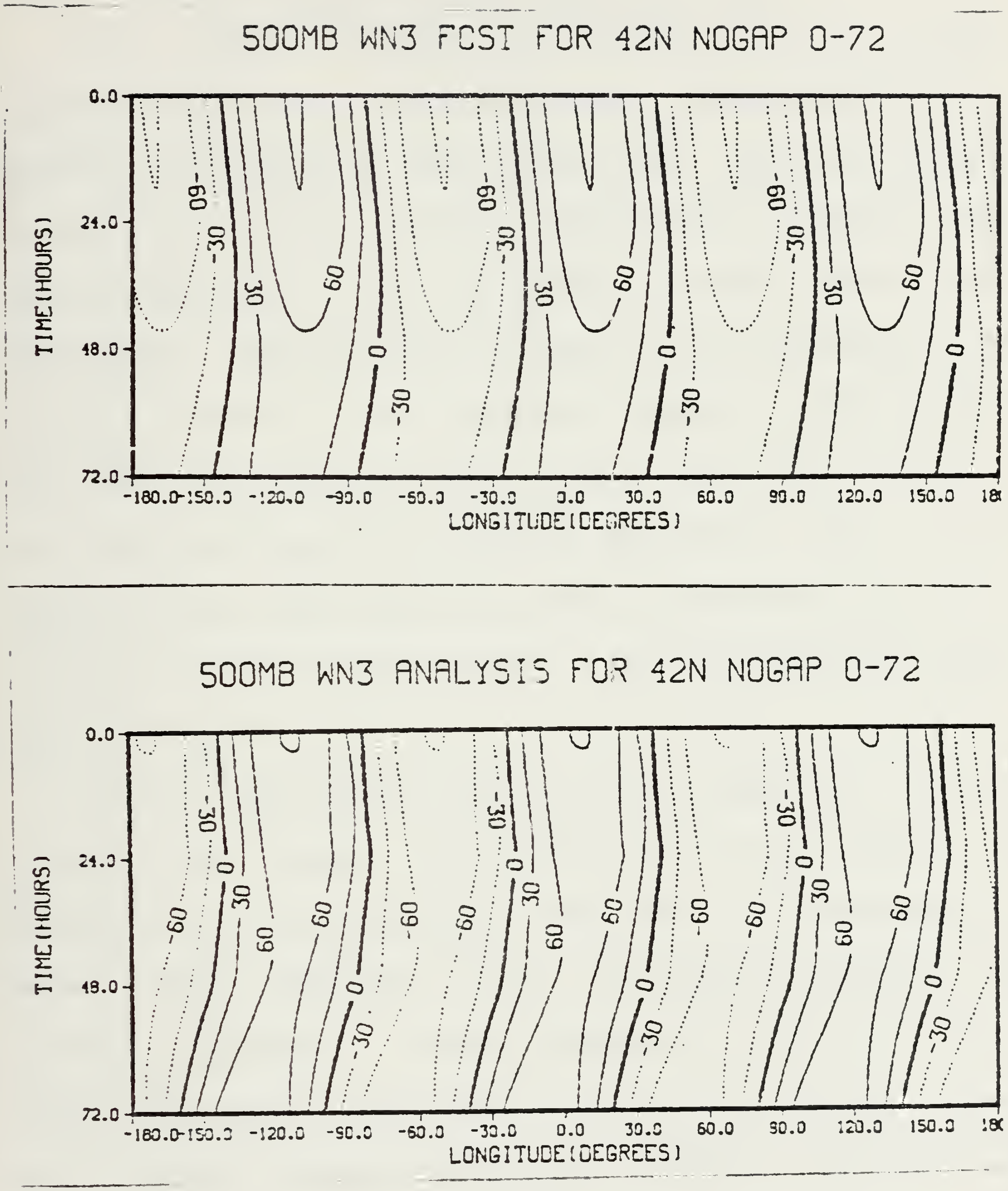

Figure 6. Hovmoller Diagrams of the Wavenumber 3 Component of the 500mb Surface Along 42N. Forecasts and Analyses are for 00Z on 18-21 Feb from NOGAPS. Intervals are 30 Meters.

represents the sum of wavenumbers 1 through 28 and, on this scale, appears to coincide with the test wave.

This analysis approach has proved to be a useful research tool when applied to forecast verification (Baumhefner and Downey,1978; Somerville,1980). Spectral decomposition of a forecast and its verification analysis allow direct comparison of the amplitude and phase speed of each wavenumber. The dimension of time further strengthens this analysis technique via a Hovmoller diagram. These trough and ridge longitude-time plots along a fixed latitude depict the time evolution of the forecast variables. Fig. 6 compares the amplitude and phase speed of successive 24, 48 and 72 hour forecasts for wavenumber 3 with the observed atmospheric behavior.

In the next chapter this and other cases will be analyzed in this manner. The harmonics of each forecast are grouped into planetary(1-3), long (5-7) and medium(8-12) waves before comparison to the verification analysis via Hovmoller diagrams. Readily discernable errors in amplitude, phase speed, development of baroclinic systems, damping of smaller scale features and planetary wave structure are just a few of the advantages of verification using spectral components.

IV. SPECTRAL VERIFICATION CASE STUDIES

In this chapter the spectral verification presented in chapter 3 will be applied to three NOGAPS forecasts, one for three days and two extending for five days. All forecasts are made from 00Z data and are verified at 24, 48, 72, 96 and 120 hour marks of the forecast.

4.1 Case 1 - February 18 to 21, 1982:

This period was selected on the basis of its pronounced planetary and long wave activity. This prediction was made with an earlier 'coarse resolution' (4 degrees lat. by 5 degrees long.) version of the NOGAPS forecast model. The spectral decomposition was applied to features along 42N averaged between 38N and 46N.

The initial 500mb pattern for case 1 was discussed in Chapter 3 and is shown in Fig. 2. Prominent features along 42N include planetary wave troughs at 160W and 45W and strong ridges at 170E, 110W and 15E, suggesting a strong wavenumber 3 component amplitude. The preponderance of ridges and troughs with wavelengths on the order of 50 to 60

degrees are the signatures of wavenumbers 6 and 7. Recall that spectral decomposition of the heights along 42N confirmed the relative dominance of wavenumber 3, 7 and 11 components (Fig. 4).

The 72-hour forecast and analysis for the 500mb surface on 21 Feb (Figs. 7a and b) appear quite similar under a cursory inspection.
The trough at 60-70W has been underforecast by the model, but overall the forecast seems to be reasonably successful. Note the excellent forecast of the two troughs in the Pacific Ocean (180W and 140W) and the strong ridge over Europe.

When the spectral decomposition is applied to the 72 hour forecast and its verification (Fig. 7c) significant amplitude differences are present. Specifically, in the planetary wave group (wavenumbers 1-3) the observed atmosphere has maintained, although to a lesser degree, the dominance of wavenumber 3 whereas the model has shifted the peak amplitude away from wavenumber 3 and into wavenumber 1. In the long wave group (wavenumbers 5,6 7) the dominance of wavenumbers 6 and 7 has shifted to the sole peak in wavenumber 7 in both the model and the analysis.

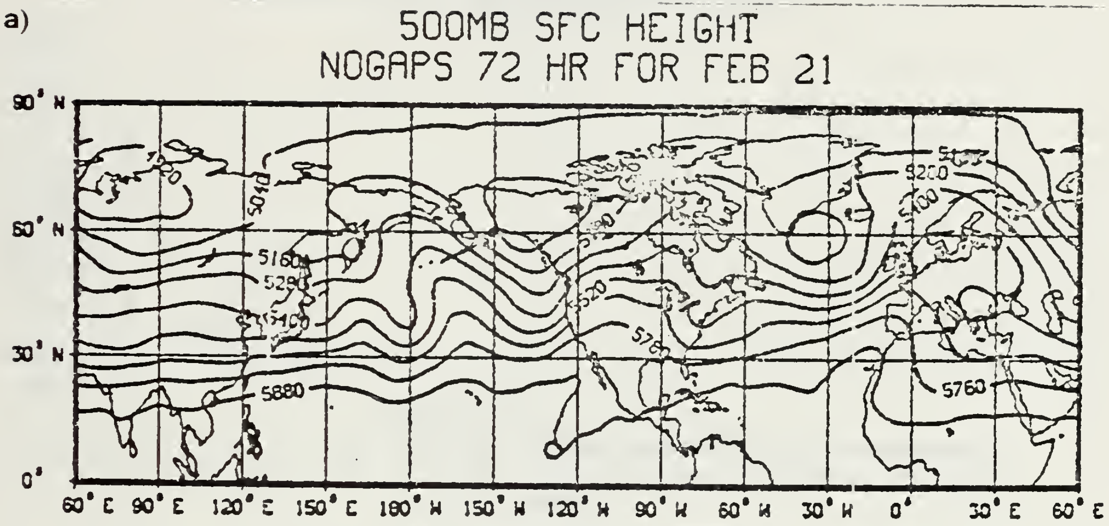

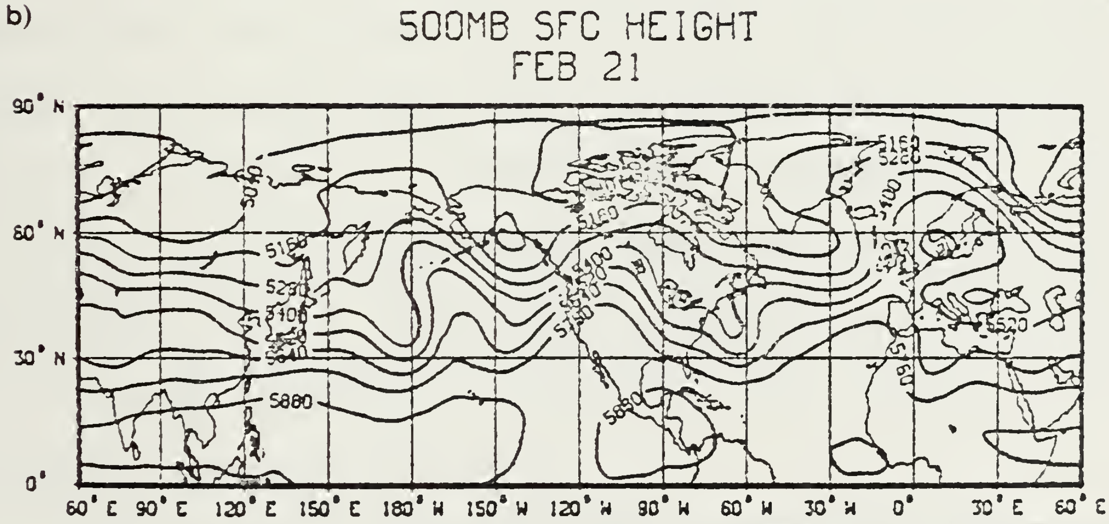

Figure 7. 500mb Heights and Wavenumber Components for 00Z 21 Feb. a) Forecast and b) Analysis with Contour Intervals of 120 Meters. c) Wavenumber Component Amplitudes in Meters.

c)

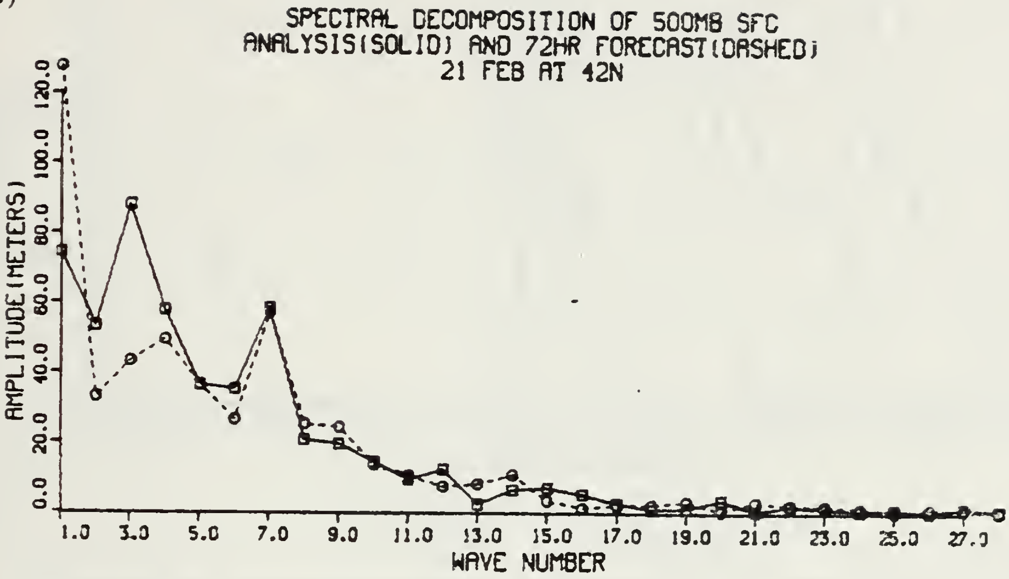

7c) Wavenumber component amplitudes.

NOGAPS accurately forecast the wavenumber amplitudes in this group. The medium wave group (wavenumber 8-12 components) initially indicates a preference for wavenumber 11, but after 72 hours the significance has shifted to the lower wavenumbers 8 and 9. This shift is slightly more pronounced in the model resulting in erroneously high forecast amplitudes for wavenumbers 8 and 9.

The Hovmoller diagrams for the planetary wave components of the forecast and the analysis (Figs. 8a and b) clearly illustrate these differences.

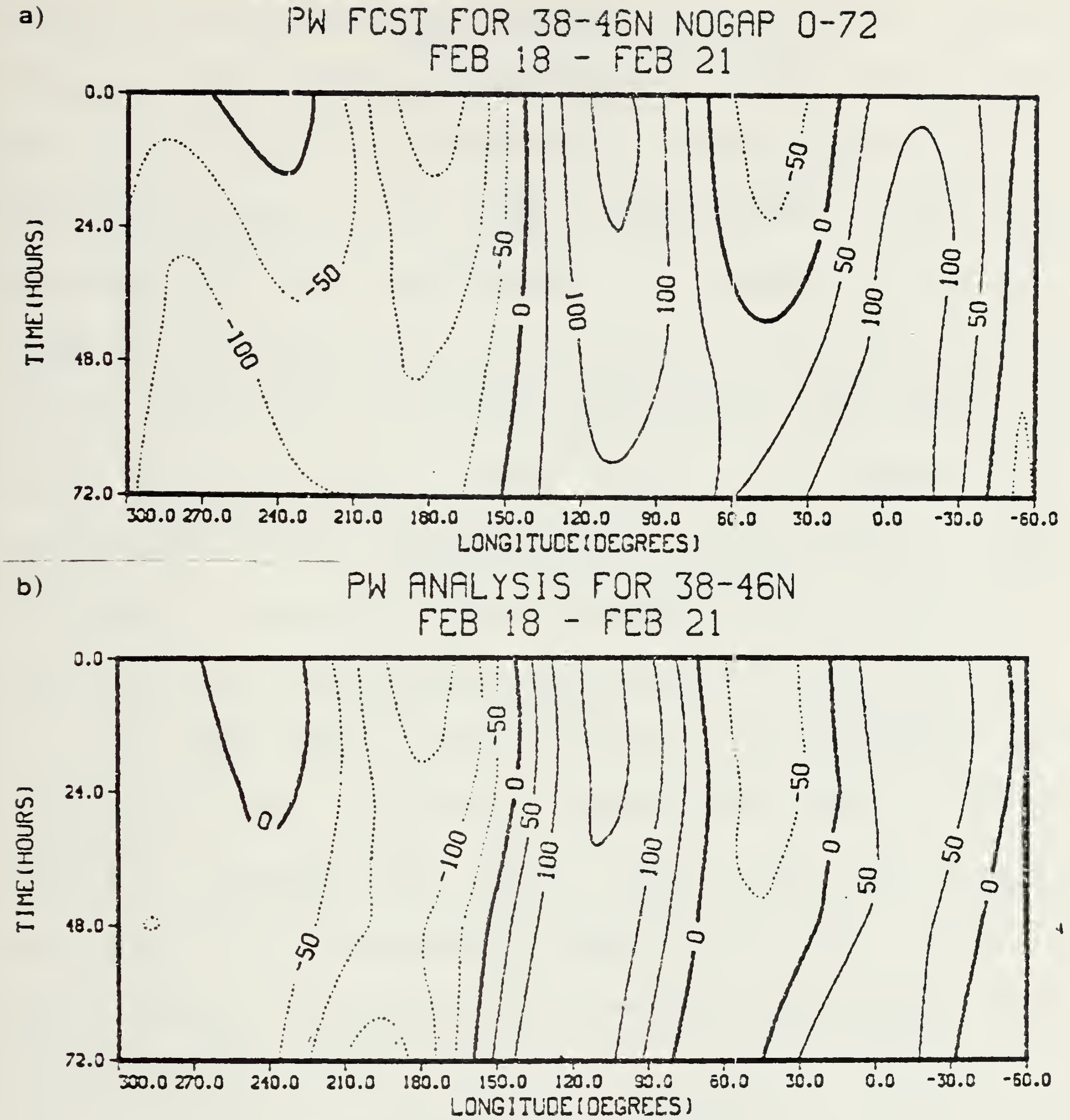

Figure 8. Planetary Wave Hovmoller Diagrams for 18-21 Feb. a) Forecast and b) Analysis with Contour Intervals of 50 Meters.

The model has accurately positioned ridges at 120W and 0, but it has underestimated the amplitude of the former by 50

meters and overestimated the latter by 50 meters. The two planetary wave troughs originating at 180W and 40W are weakened too rapidly in the forecast and become distorted by the spurious formation of a deep trough at 90E. The trough originating at 30E also weakened too rapidly to the point where it is higher than the mean height and is only a trough in the sense that it is between two ridges. The other prominent feature is the forecast trough at 90E which has no counterpart in the observations. The seemingly random changes in trough and ridge intensity form a pattern when the differences in component amplitudes are considered.

The NOGAPS 72-hour forecast shows the wavenumber 1 signature emerging with general ridging from 150W to 40E and general troughing from 40E to 150W while the analysis depicts more of a wavenumber 2 and 3 signature. Figs. 9a and b compare the forecast and observed wavenumbers 1 and 3 individually.

NOGAPS forecasts wavenumber 1 to be 70% more intense than the observation while underforecasting wavenumber 3 by 55%. Despite the presence of wavenumbers 2 and 3, the planetary wave characteristics in the 72 hour NOGAPS forecast are largely determined by the overwhelming dominance of

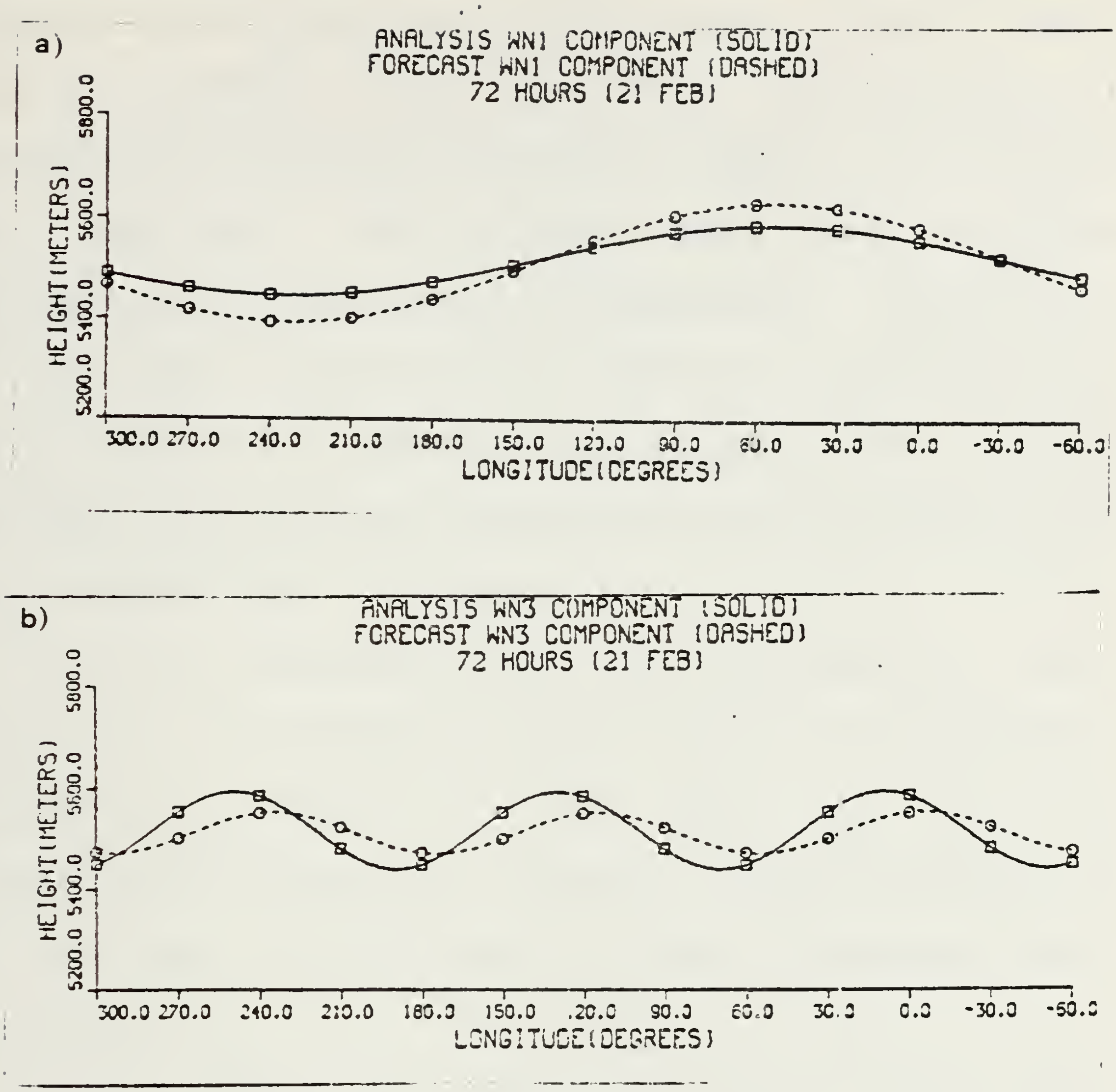

Figure 9. Wavenumber 1 and 3 Components for Case 1. a) Wavenumber 1 Component for Analysis (Solid) and Forecast (Dashed) for 00Z 21 Feb. b) Same as a except for Wavenumber 3 Component.

wavenumber 1. Erroneously low heights, troughs too strong and ridges too weak, exist in the region of 60E to 120W and erroneously high heights, troughs too weak and ridges too

strong, exist in the region of 120W to 60E. Synoptic examples of the effect of the reduction of the wavenumber 3 component are evident in the ridge at 120W and the trough at 60W. From 150W to 110W the model underforecasts the ridge in this area and smooths out its amplitude. From 110W to 60W the model overforecasts the height of the eastern side of the ridge and smooths out the trough at 60W. These amplitude errors are also evident in other regions of the 72 hour forecast (Figs. 7a and b).

The long wave group verifies the wavenumber 5,6 and 7 components. The general agreement between the individual wavenumber amplitudes in this group (Fig. 7c) through the 72-hour period consequently produces a general agreement in the amplitudes of their respective Hovmoller diagrams (Figs. 10a and b).

This diagram shows seven troughs and ridges at 72 hours signifying the dominance of wavenumber 7. In this grouping a region of maximum amplitude (contour intervals are 15m) is evident between 180W and 30W in both the model and the observation. There is strong agreement between the forecast and observed long waves in the Hovmoller diagrams showing NOGAPS performing well at this scale.

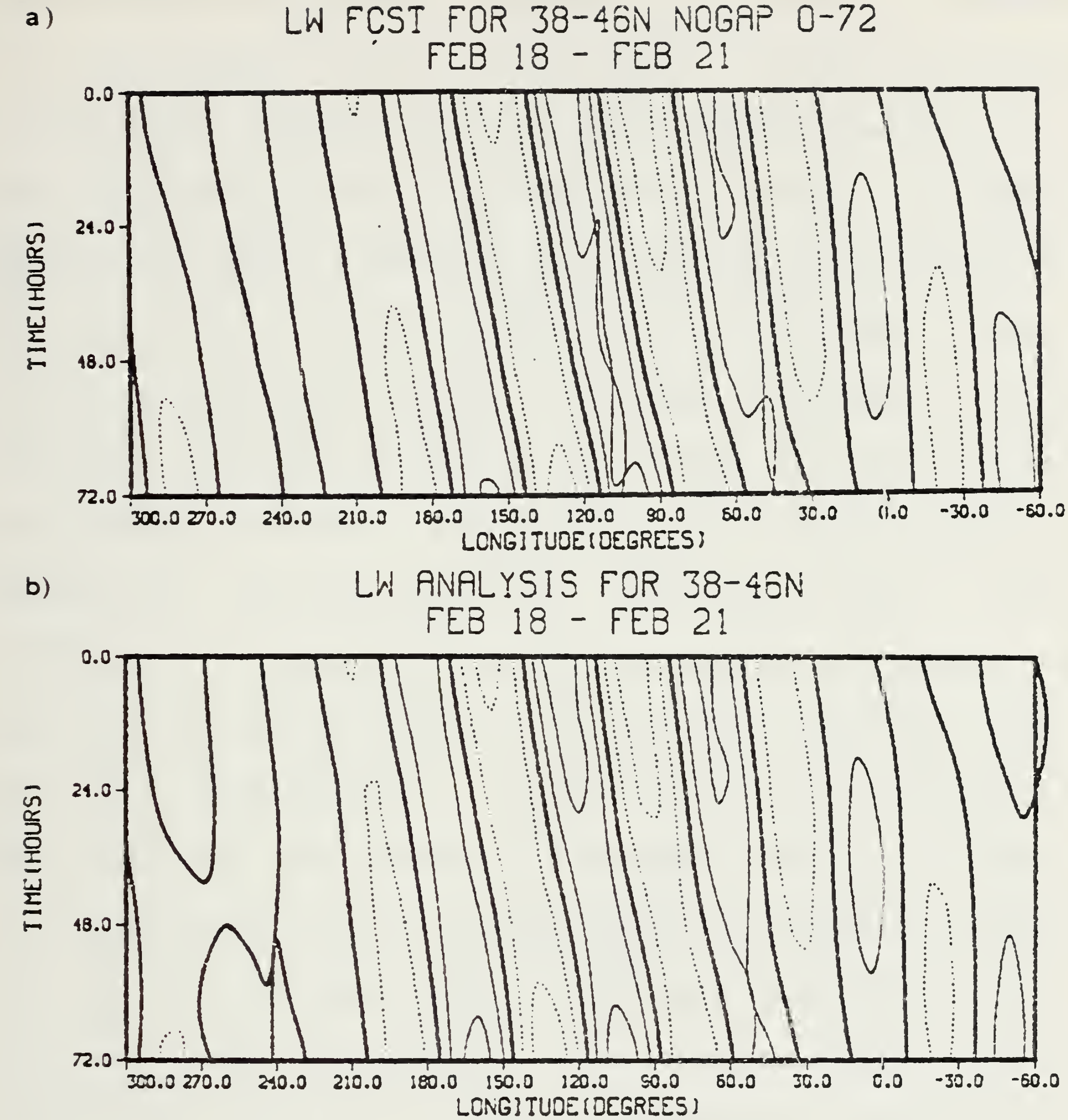

Figure 10. Long Wave Hovmoller Diagrams for 18-21 Feb. a) Forecast and b) Analysis with Contour Intervals of 30 Meters.

The interaction of wavenumbers 8 through 12 in the medium wave group creates a complex pattern in the analysis

and forecast trough-ridge diagrams. The Hovmoller diagrams for the forecast and observation (Figs. 11a and b) both show eleven waves initially and nine waves after 72 hours. The amplitudes (contour intervals are 10 meters) and phase speeds can still be compared, but the errors are more difficult to trace. The model shows an erroneous loss of amplitude, particularly evident at 48 hours. However, at 72 hours the increased activity in the region from 140E to 120W is properly forecast. The phase speed is approximately 10 degrees too fast in the region from 00E to 120E. Conversely, the model has done extremely well in forecasting the speed of the wave features between 140E and 150W. Overall, the model exhibits reasonable success for both the amplitudes and phase speeds of the medium waves at 72 hours. It is important to note the amplitude of the medium wavenumbers is often smaller than the planetary wavenumbers by as much as an order of magnitude. Also as wavenumbers increase to the point where they cannot be accurately represented by the model's horizontal resolution, the spectral decomposition is less accurate as well.

The results of Case 1 indicate NOGAPS erroneously shifted the planetary wavenumber dominance from wave 3 and

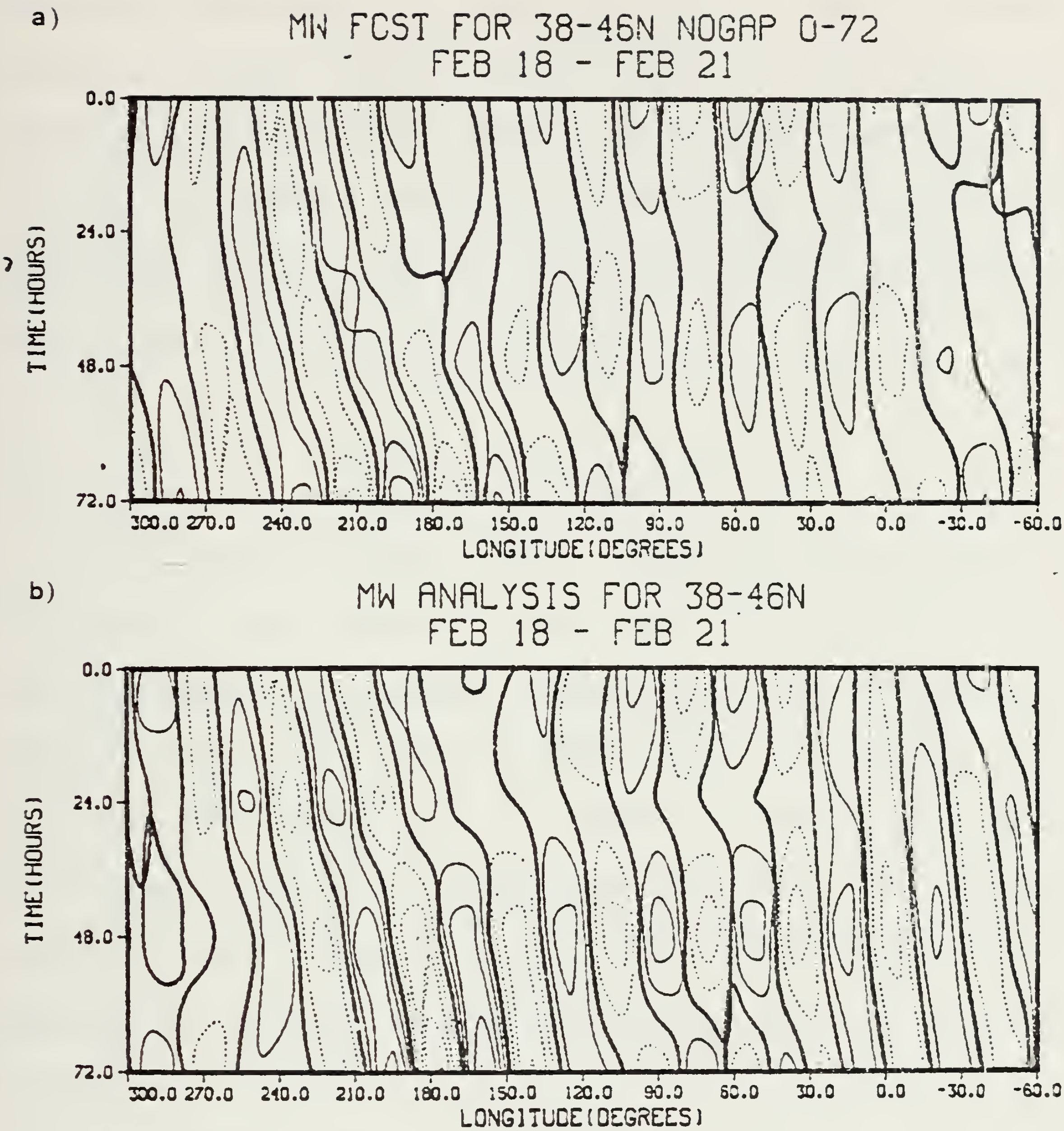

Figure 11. Medium Wave Hovmoller Diagrams for 18-21 Feb. a) Forecast and b) Analysis with Contour Intervals of 15 Meters.

into wave 1. Due to a difference in wavenumber signatures, accurate planetary wave phase speed comparisons between the

model and the observation were difficult. Both the amplitudes and phase speeds of the long waves were accurately predicted by the model. NOGAPS showed some loss of amplitude in the medium waves and shifted peak amplitude from wavenumber 11 to 8 and 9. The phase speed errors of the medium waves as a group were small.

4.2 Case 2 - October 06 to 11, 1982:

This period provides a good example of the formation of an intense ridge (blocking high) over the western U.S. and was discussed in the NOAA, Western Regional Attachment of October, 1982. For this case NOGAPS horizontal resolution is 2.4 degrees of latitude by 3. degrees of longitude interpolated onto a 2.5 by 2.5 degree spherical grid. The spectral decomposition is applied to the height of the 500mb surface along 45N (averaged between the heights given at 42.5N and 47.5N).

The 500mb heights, depicted from 30N to 60N, for 06 Oct in Fig. 12a shows a fairly zonal pattern from the east coast of Asia to the Eastern Atlantic.

Note the ordinate/abscissa ratio is more than one. This distortion produces a visual magnification of the amplitudes

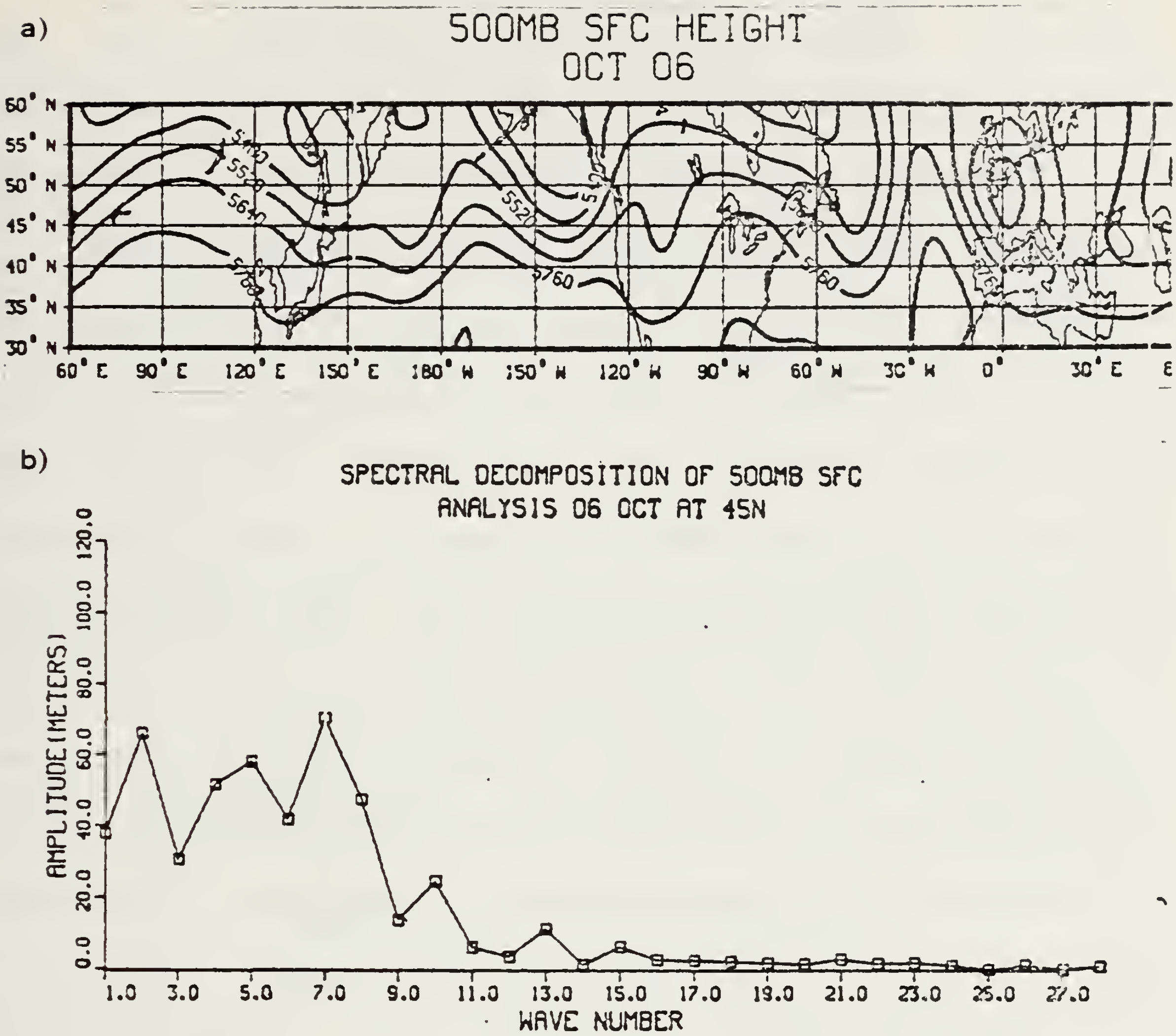

Figure 12. 500mb Heights and Wavenumber Components for 06 Oct. a) 500mb Heights with Contour Intervals of 120 Meters. b) Wavenumber Component Amplitudes in Meters.

of each wave. This scale was chosen for clarity and is maintained throughout this and the remaining cases. Prominent ridges are located at 20W and 30E and the flow splits

at 10W. Spectral decomposition (Fig. 12b) shows wavenumber 2, 5 and 7 components are dominant initially. The zonal character of this case is shown by the relatively even distribution of amplitudes among wavenumbers 1 through 8.

Seventy-two hours later (Fig. 13a) a deep trough has developed over the central U.S. and prominent ridges have rapidly developed over the western and eastern U.S. coasts. The model (Fig. 13b) does not adequately forecast the strength of these features. A comparison of the spectral decomposition (Fig. 13c) of the analysis and the forecast at 72 hours shows a marked increase in the dominance of the wavenumber 2 and 7 components of the atmosphere while the model incorrectly smoothed the amplitude of wavenumber 2 but correctly maintained the relative strength of wavenumber 7.

At the 120 hour mark (11 Oct) of the forecast period both the eastern and western U.S. ridges have continued to strengthen (Fig. 14a). The model shows an ability to properly forecast the phase speed of the wave features such as the troughs at 170W and 40W and the ridge at 160E but continues to underestimate the strength of the ridges (Fig. 14b) over the U.S. Spectral decomposition of the observation shows the largest amplitudes are in wavenumbers 2, 3, 4

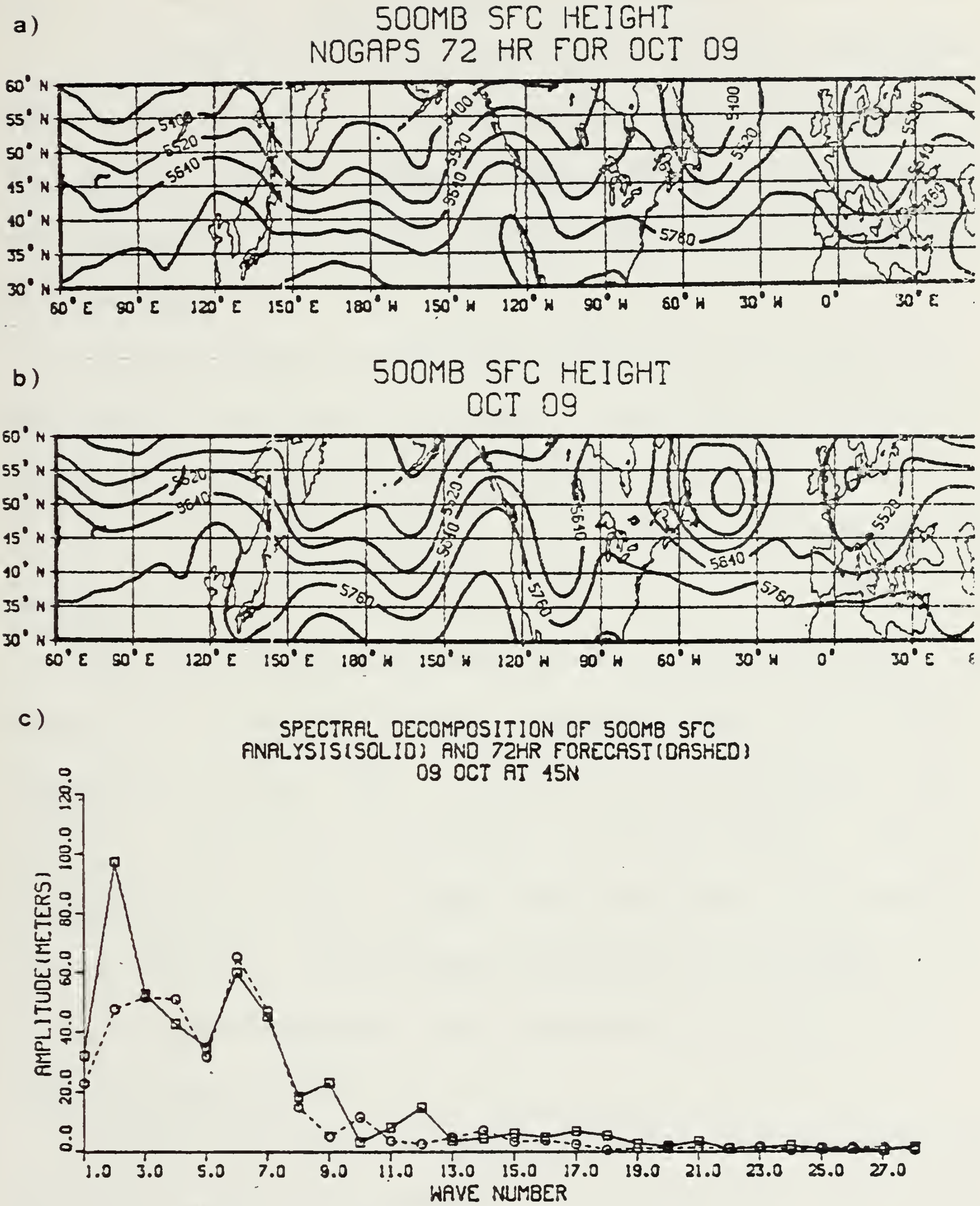

Figure 13. Same as Fig.7 except for 09 Oct.

and 5 all having similar values (Fig. 14c). Meanwhile the model has shifted the dominance to wavenumber 4 while keeping the amplitude of wavenumbers 5 and greater relatively small. The largest amplitude changes in the model during the forecast period occurred in wavenumbers 2, 3 and 4 while the atmosphere additionally showed large amplitude changes in wavenumber 5.

The significance of the amplitude errors is readily discernable in the Hovmoller plots. Initially both of the planetary wave trough-ridge diagrams (Figs. 15a and b) exhibit the characteristics of a large wavenumber 2 component.

After 72 hours the observation has greatly increased the strength of the wavenumber 2 signature while the forecast decreased it (Fig. 16a). The model has successfully forecast the strength of the trough at 180W (-135m), but the strength of the other trough and both ridges are severely underestimated. The combined dominance of wavenumbers 2 and 3 in the NOGAPS forecast has introduced a spurious ridge at 0W and trough at 50E.

By 120 hours the atmosphere exhibits maximum amplitude in the planetary wavenumbers 2 and 3 (Fig. 14c). This shift

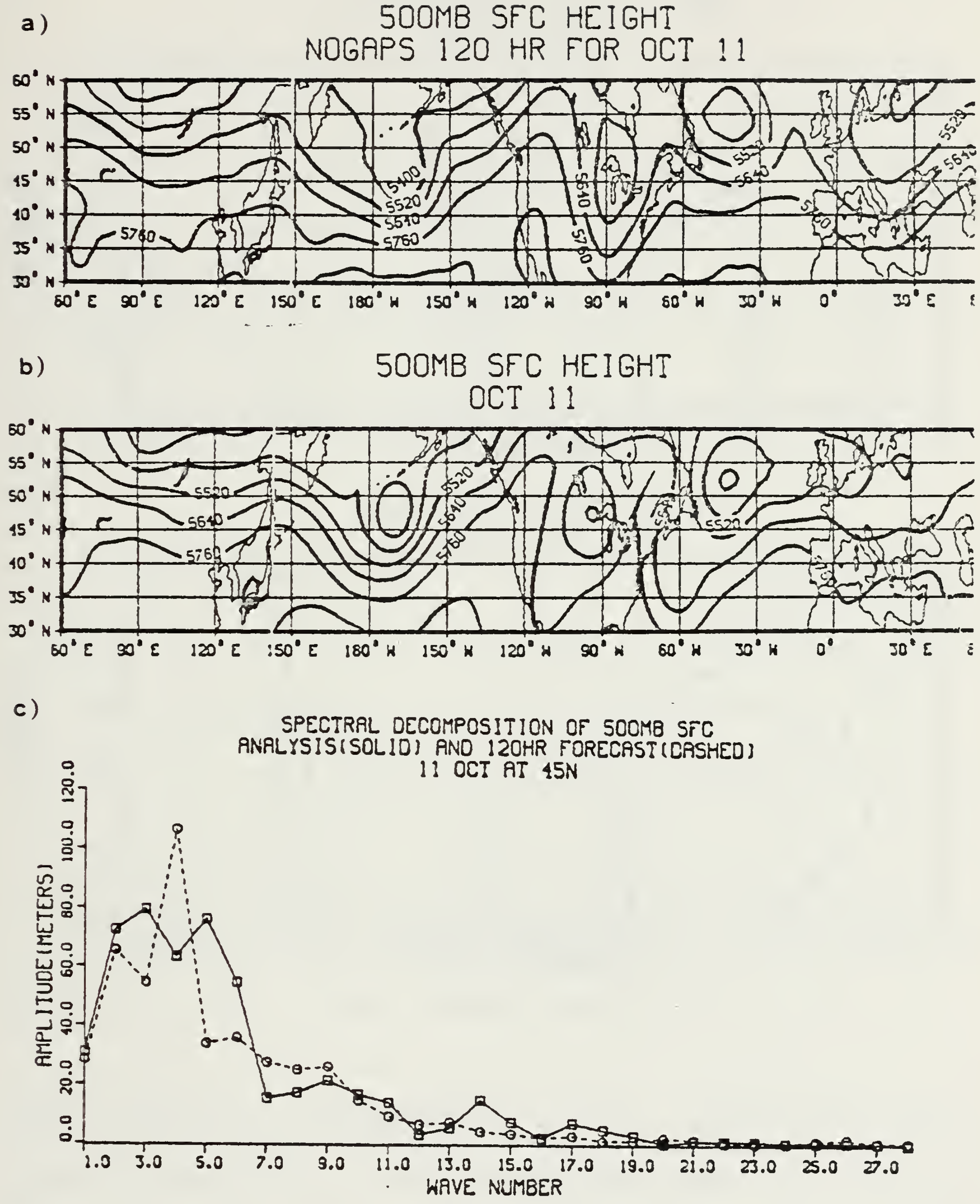

Figure 14. Same as Fig.7 except for 11 Oct.

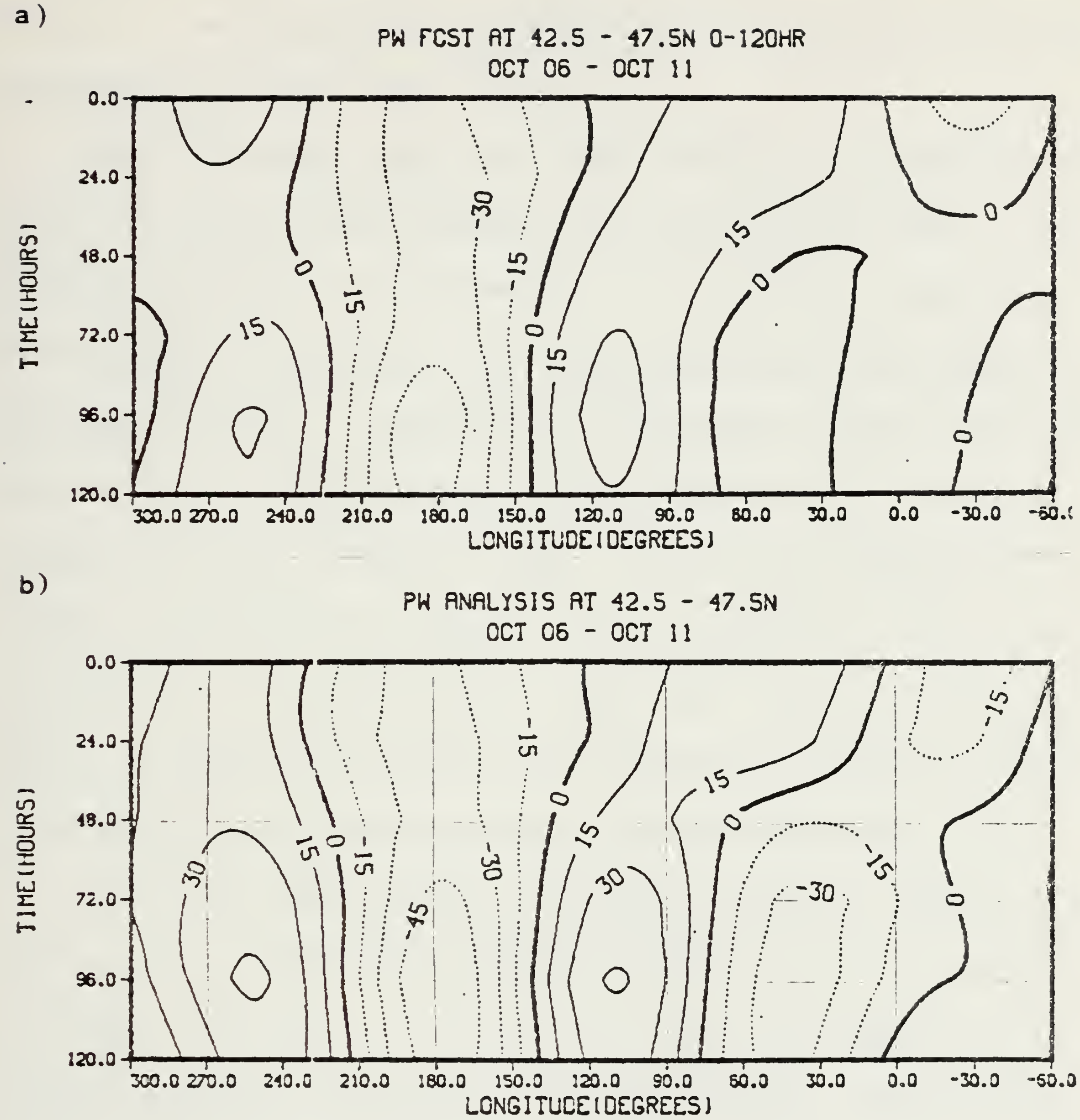

Figure 15. Same as Fig. 8 except for 06-11 Oct.

has not affected the amplitudes of the planetary wave features as much as it has sharply tightened the spacing between the troughs and ridges producing more of a

wavenumber 3 signature. The model has forecast the amplitude of wavenumber 1 accurately while underestimating wavenumber 3 by 30% (Fig. 16b).

Thus the model has once again failed to predict the shift and erroneously smoothed the highest amplitudes. The model's planetary wave Hovmoller diagram shows the weaker amplitudes at 120 hours and, significantly, the resultant smoother pattern. Specifically the ridges at 105E and 110W are too low and the trough at 45W is too high. Synoptically these errors are evident in Fig. 14b as the failure of the model to adequately forecast the strength of the ridge building on the west coast of the U.S. and the trough at 40W. The general placement of comparable features is good especially in the Pacific region near the dateline.

The long wave component Hovmoller diagrams (Figs. 17a and b) show NOGAPS successfully forecasting the long wave features. Overall the forecast has accurately predicted the general regions of high long wave amplitudes, 120W to 90E, and low long wave amplitudes, at 90E to 120W. Observed long wave amplitudes are more intense than the forecast after the 72 hour mark. Comparison of model and observed phase speeds shows NOGAPS to be fast, particularly in the high amplitude

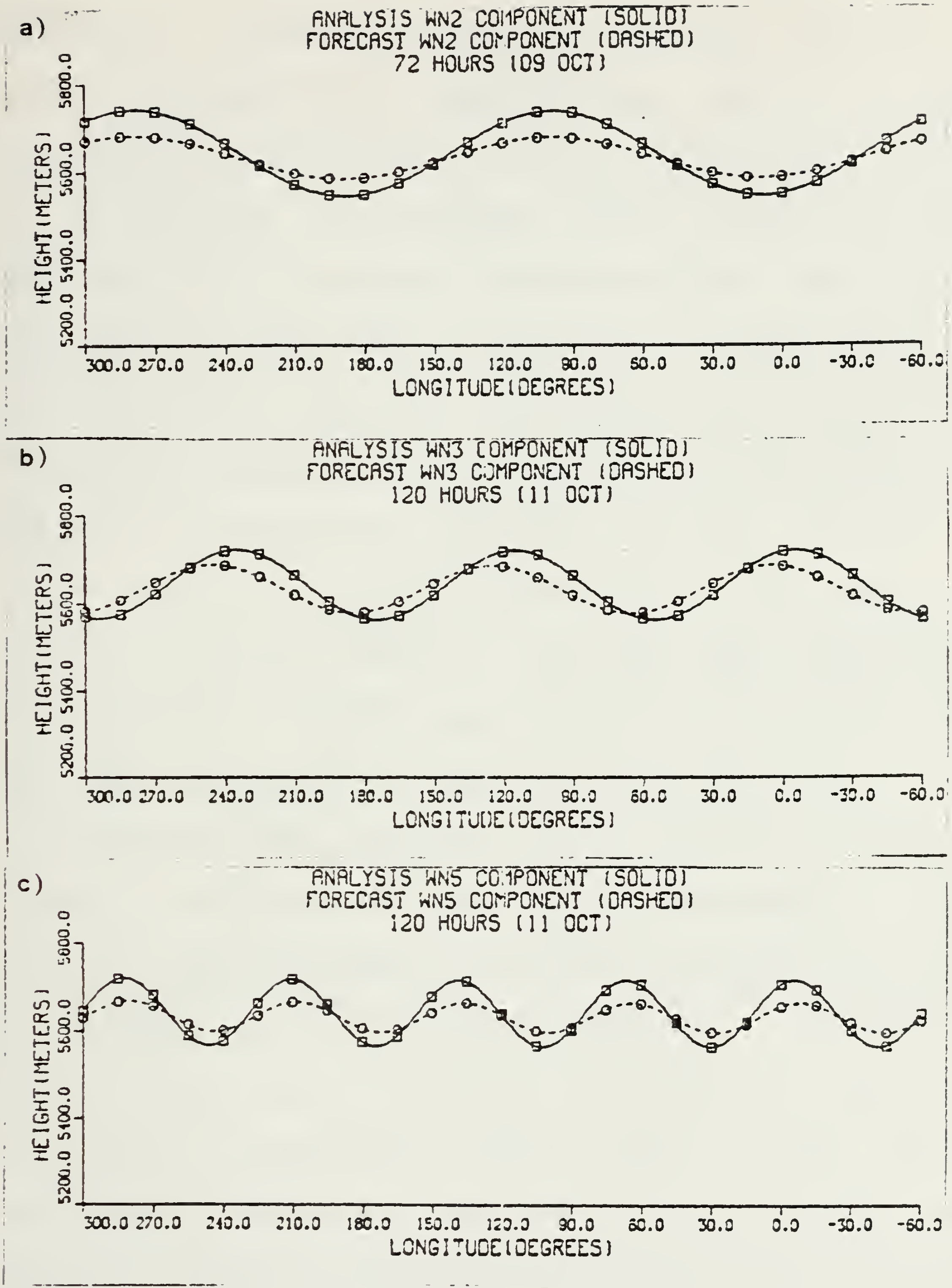

Figure 16. Wavenumber 2, 3 and 5 Components for Case 2. Same as Fig. 9 except a) Wavenumber 2 for 09 Oct, b) Wavenumber 3 for 11 Oct and c) Wavenumber 5 for 11 Oct.

waves between 120W and 30W. The shift of the atmosphere to wavenumber 6 signature within the group by 72 hours was properly forecast by the model and wavenumber 5, 6, and 7 components have less than 10% amplitude error (Fig. 13c).

By 120 hours the atmosphere shows maximum long wave amplitude in the wavenumber 5 component (Fig. 14c) and the Hovmoller plot (Fig. 17a). In contrast the model (Fig. 17b) exhibits small long wave amplitudes and underestimates wavenumber 5 by more than 50% (Fig. 16c) and wavenumber 6 by 30% while overestimating wavenumber 7 by 60%. The result of these errors is a general smoothing of all ridges and troughs. Also the region of high amplitude, 120W to 90E, has exhibited slow phase speed error while the region of low amplitude, 90E to 120W, showed rapid phase speed.

The medium wave components (Figs. 18a and b) begin the forecast period with the signature of wavenumber 8. By 72 hours no clear wavenumber preference is present in either the forecast or the atmosphere. The same is true after 120 hours. The initial significant amplitudes of these waves are lost in the atmosphere after 24 hours. A few, such as the trough originating at 140W and the ridge at 120W, maintain their amplitude throughout most of the five day period.

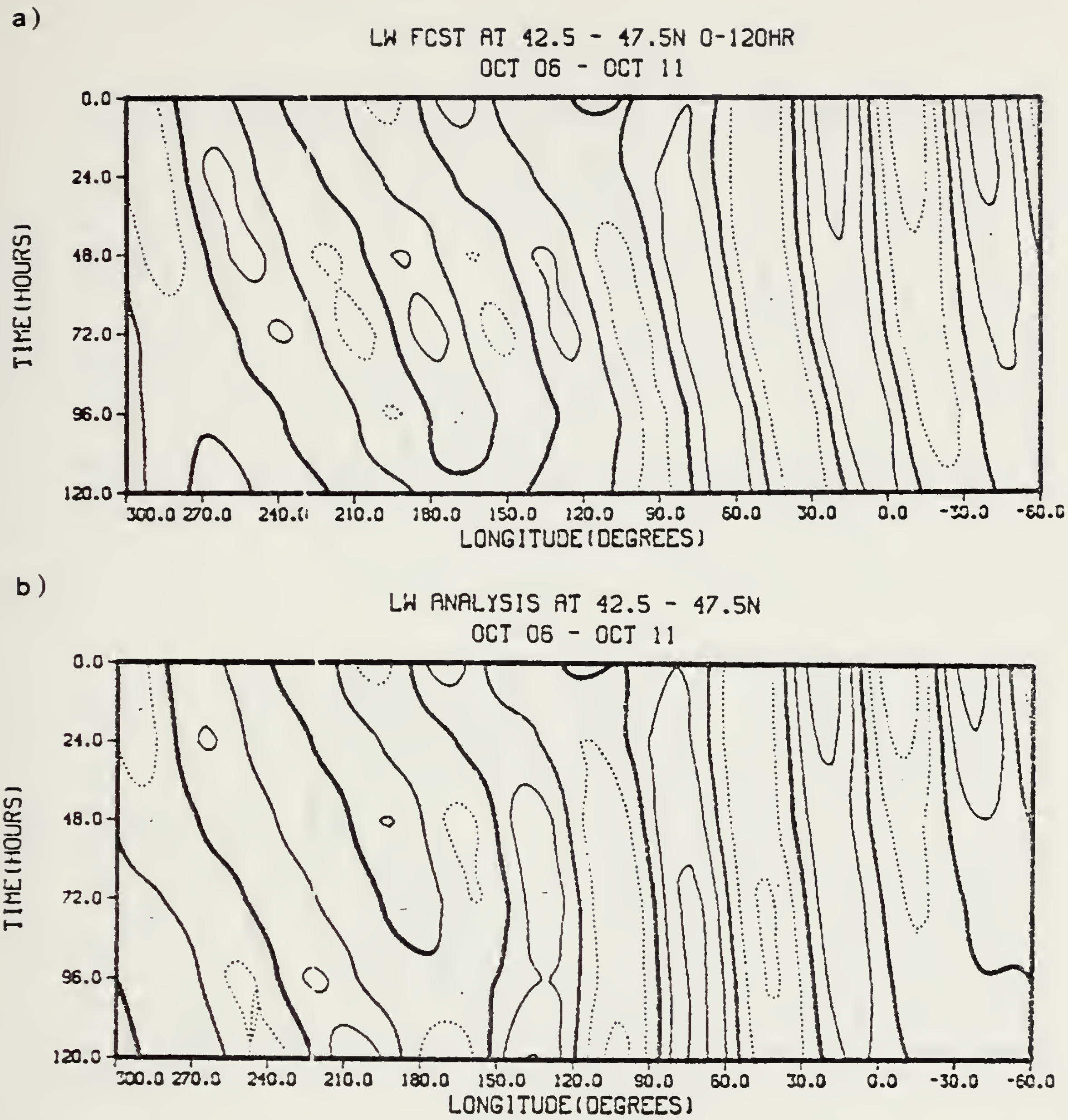

Figure 17. Same as Fig. 10 except for 06-11 Oct.

At 120 hours new activity appears in the region from 180W to 60W. The model dampens all the wave features after 24 hours which is erroneous in the case of the trough-ridge

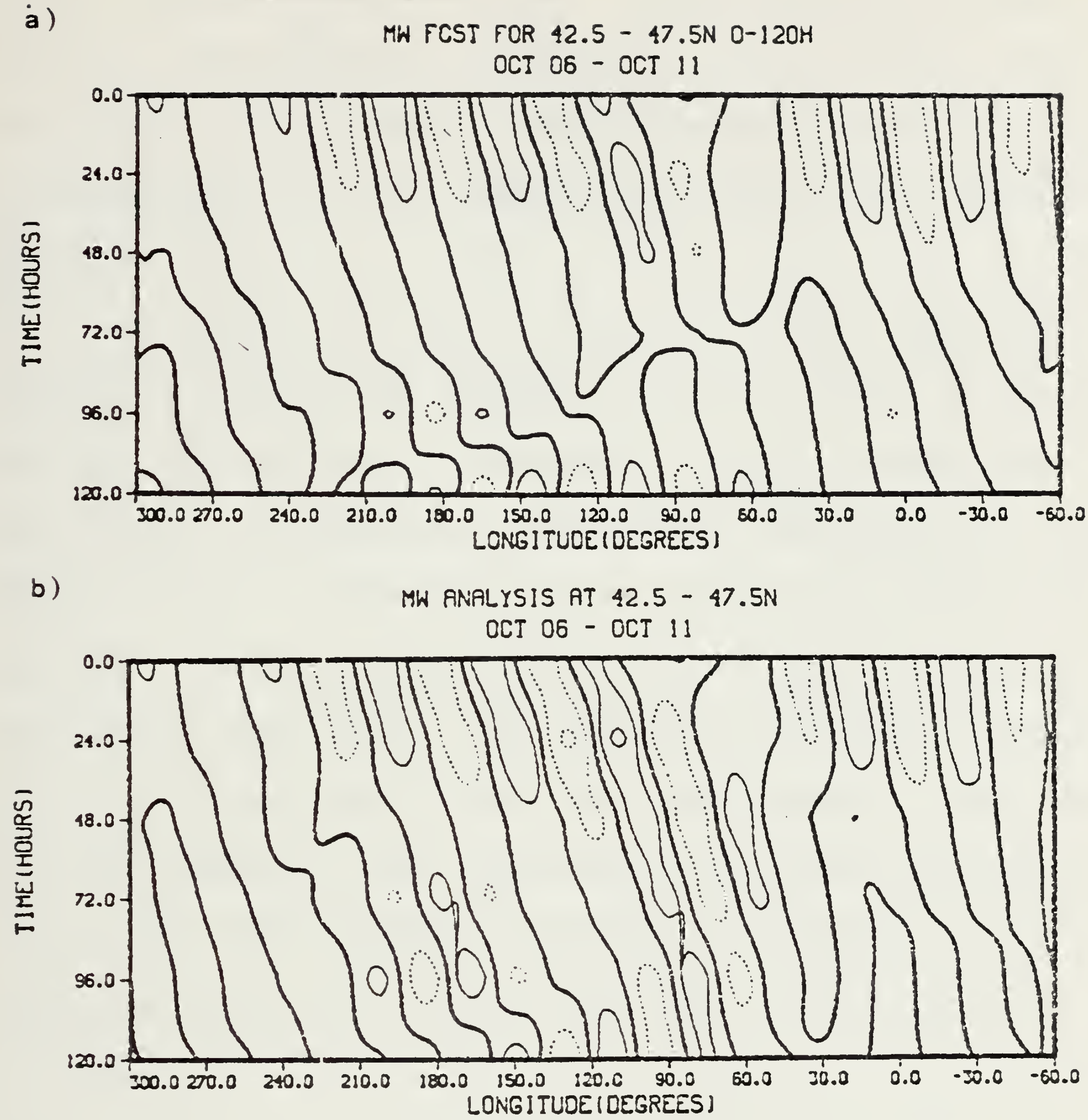

Figure 18. Same as Fig. 11 except for 06-11 Oct.

system over the western U.S. The model does capture the new activity at the five day mark. An overall comparison suggests a phase speed error of 5-10 degrees too fast where

direct comparisons can be made. Synoptically this difference is not visible on the scale of Figs. 14a and b but would show up as a slightly rapid movement of features with a wavelength of 30 to 45 degrees over the 120 hour forecast period.

The results of Case 2 indicate NOGAPS erroneously smoothed a shift in the planetary wave activity at 72 hours and again at 120 hours. Planetary wave phase speed errors were small for comparable features and negligible in the Pacific region. Although long wave forecast amplitudes were smoothed, NOGAPS correctly produced two distinct regions of contrasting amplitudes. Phase speeds were slightly too fast in the high amplitude region but satisfactory in the low amplitude region. The amplitudes of the medium wave features were well forecast, but showed a fast bias in wave speed and several key features were lost in the forecast.

4.3 Case 3 - October 22 to 27, 1982:

During this forecast period the 500mb surface changed from a predominantly long wave flow pattern to a more zonal situation. In particular the region from 150E to 140W underwent the breakdown of a blocking ridge. Again the

NOGAPS horizontal resolution is 2.4 degrees lat. by 3 degrees long. interpolated onto a 2.5 by 2.5 degree spherical grid. The spectral decomposition is applied to the heights along 45N averaged between 42.5N and 47.5N.

The 500mb heights from 30N to 60N for 22 Oct (Fig. 19a) includes prominent troughs at 60E, 125E and 140W with lesser troughs at 75W and 15W.
Noteable ridges exist at 90E, 170E, 110W, 45W and 20E. The wavenumber 5 dominance is clearly present in Fig. 19b along with strong amplitude components of wavenumbers 3 and 4 due to their particularly strong trough-ridge systems.

After 72 hours amplitude differences are already apparent between the 500mb patterns of the model and the analysis (Figs. 20a and b). The model has underforecast the strength of the ridges at 90E and 35E and the troughs at 70E, 140E, 140W and 10E. The only obvious NOGAPS overforecast is in the ridge at 100W.

The individual wavenumber components (Fig. 20c) at 72 hours show the dominance remains with 4 and 5. Large amplitude increases have occurred in wavenumbers 1, 7, 9 and 10 and large decreases at 2 and 3. The model has accurately predicted most of the changes but consistently

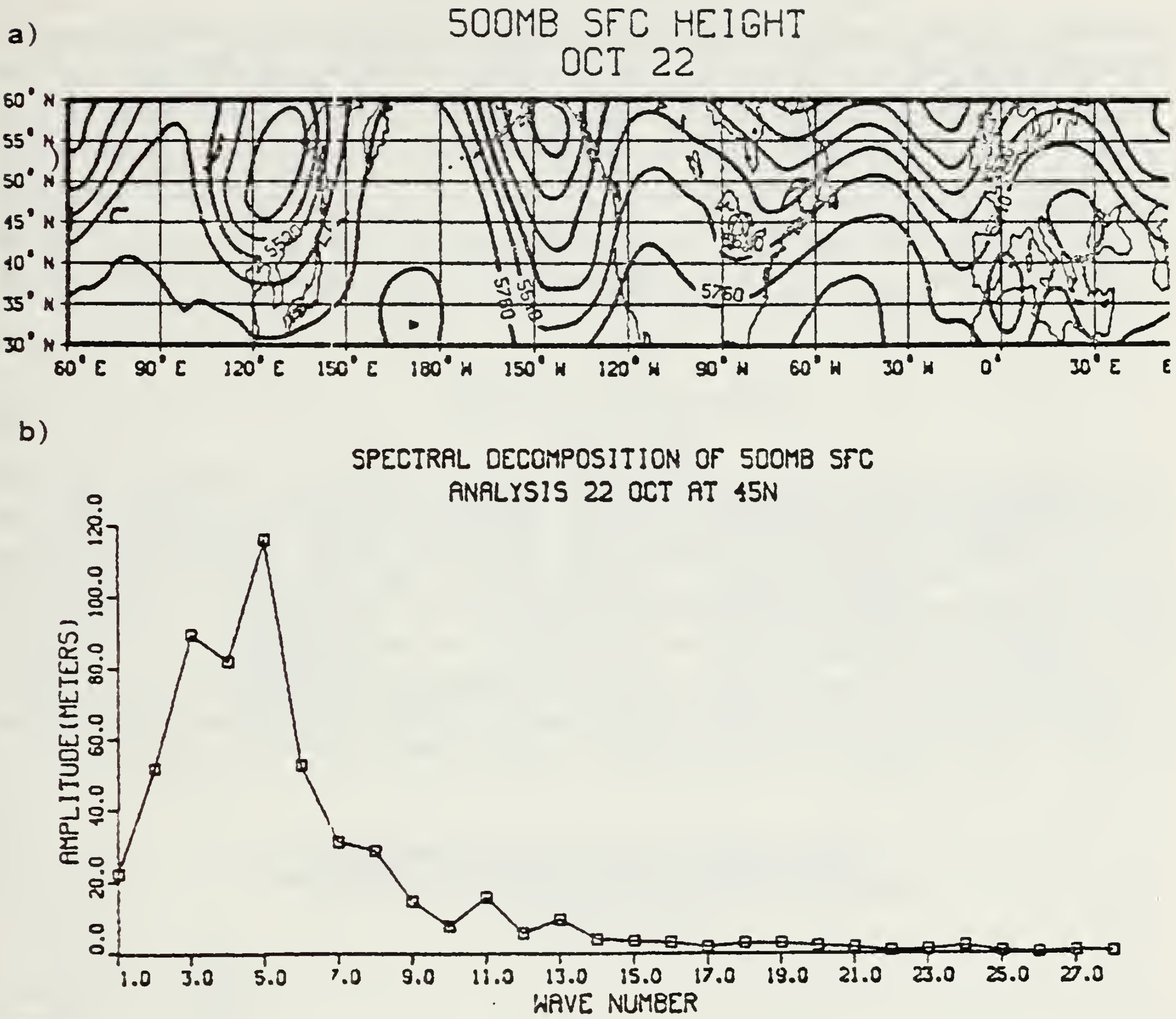

Figure 19. Same as Fig. 12 except for 22 Oct

underestimates the strength of wavenumbers 6 through 10. In terms of this study's wave groupings the amplitudes of the planetary waves are forecast very well, the long waves are too weak by 10 to 20% and the medium waves are too weak by 30 to 40%.

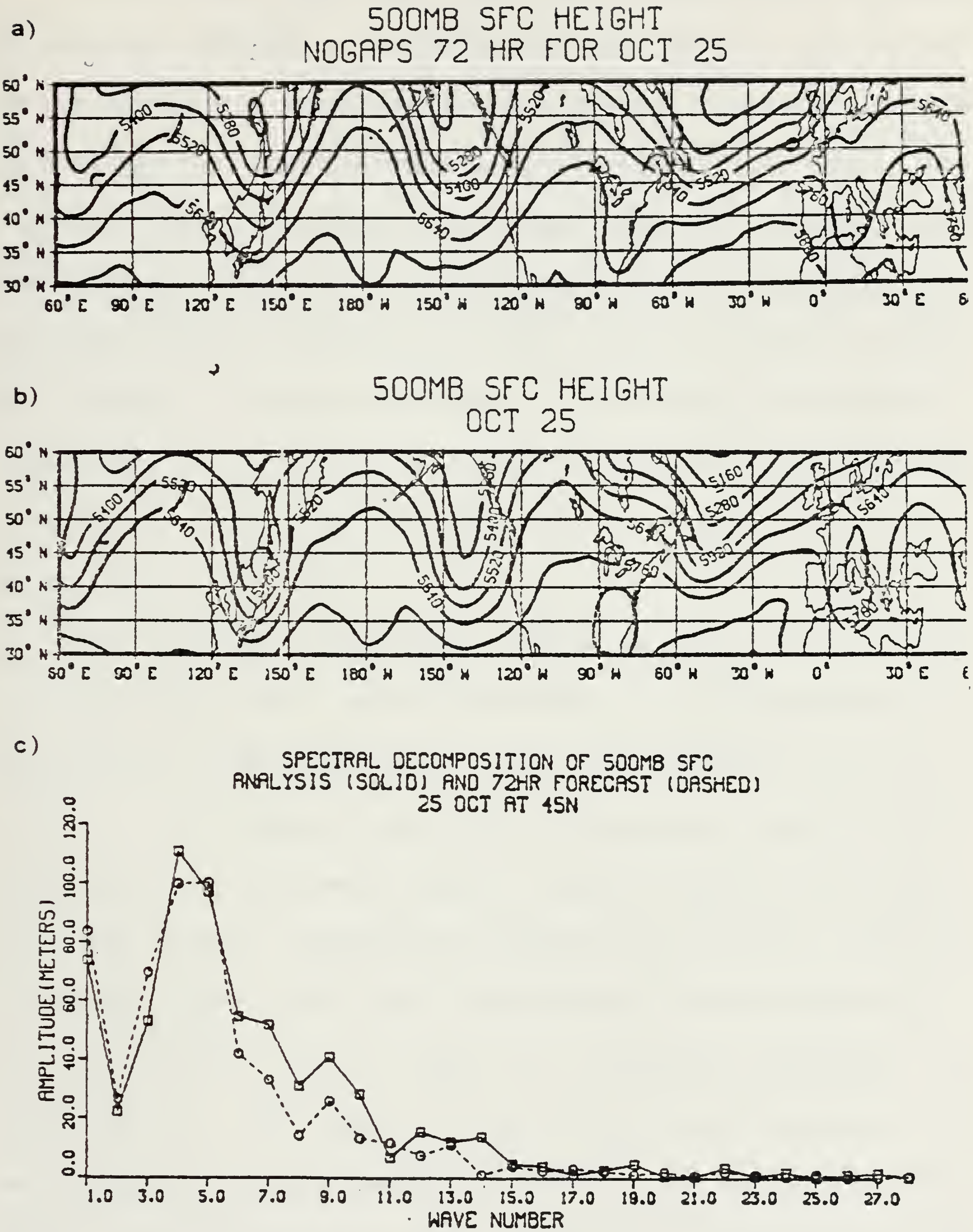

Figure 20. Same as Fig. 7 except for 25 Oct

At the 120 hour mark both phase speed and amplitude errors are evident in the 500mb patterns (Figs. 21a and b). Phase speeds are consistantly too rapid. Examples include the trough at 75E (10 degrees of longitude too fast), the ridge at 180W (15 degrees too fast) and the trough at 40W (25 degrees too fast). The amplitudes of the trough at 160E and the ridge at 180W are too weak and the ridge at 95W is too strong. A ridge has formed in the region from 160W to 120W which has aided in the weakening of the blocking ridge at 180W. The model has missed this important feature entirely.

The individual wavenumber components (Fig. 21c) at the 120 hour mark show a general decrease in all amplitudes with especially large percentage drops in wavenumbers 3, 4, 5, 6 and 7. The relative dominance of planetary waves is much smaller now, but there exists a distinct peak at wavenumber 4. The model's wavenumber components also show a general decrease in amplitudes with significant errors occurring in 3, 4, 8, 9 and 12 while the dominant wavenumber is wavenumber 3. In terms of this study's wave groupings the amplitudes of the planetary waves are too strong by 20 to 30%, the long waves are well forecast and the medium waves are too weak by 30 to 40%.

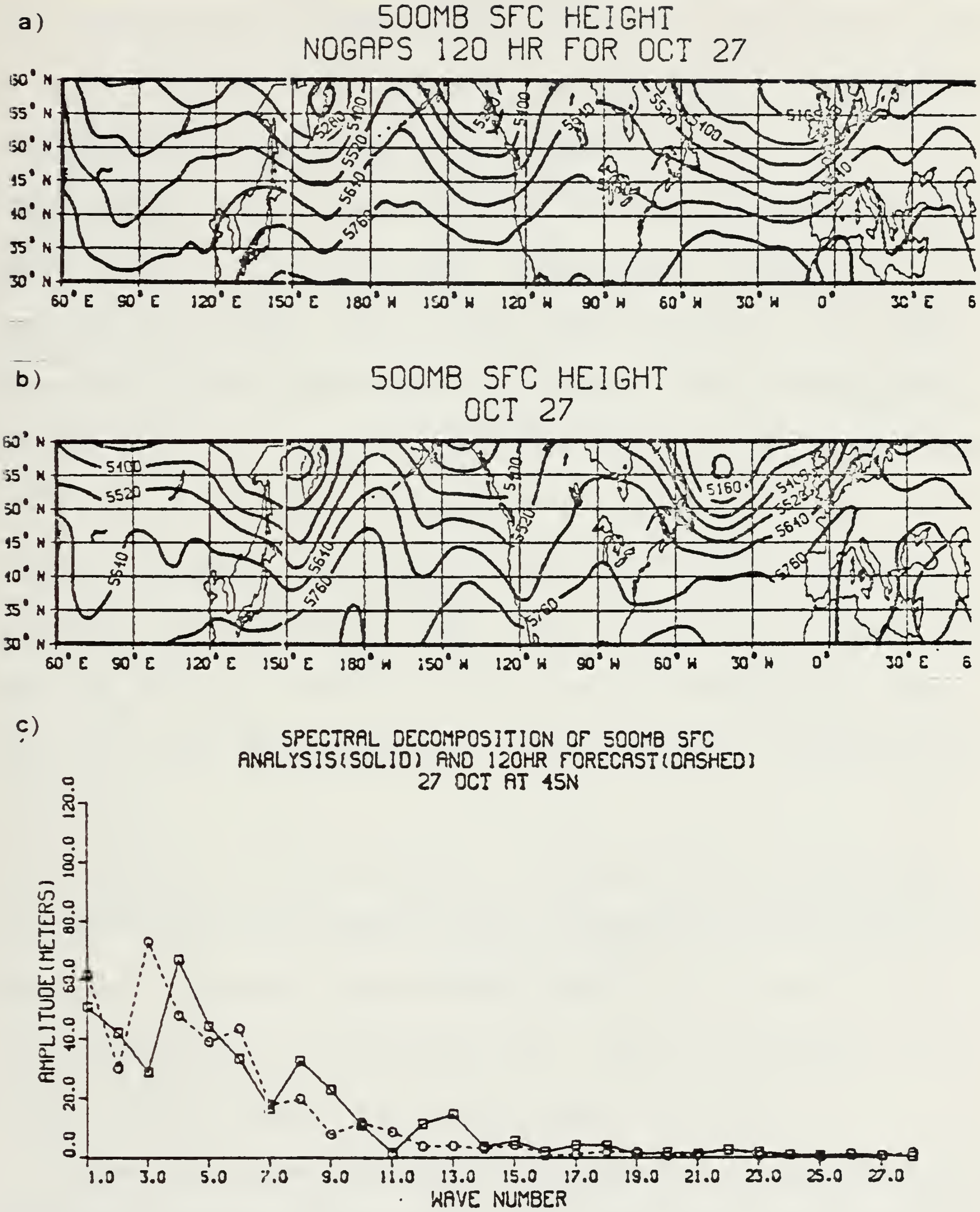

Figure 21. Same as Fig. 7 except for 27 Oct

The Hovmoller diagrams for the planetary wave components of the forecast and the analysis (Figs. 22a and b) both show a shift from the sole dominance of wavenumber 3 to a shared dominance with wavenumber 1 by 72 hours.

The forecast phase speed error of the model is negligible at this point. The wavenumber 3 features are forecast too strong as a result of the 20% overforecast by the model. Examples include the troughs at 110E and 150W and the ridges at 80W and 30E. At 120 hours the model shifts its maximum activity to wavenumber 3 while the atmosphere shows a distinct wavenumber 1 signature. Now the NOGAPS wavenumber 3 features, the troughs at 120E, 60W and 35E and the ridges at 85W and 35E, are much too strong. Fig. 23 graphically presents the 100% overforecast of the wavenumber 3 component by the model.

The positions of the ridges at 85W and 35E are excellent, but the trough at 120E has been erroneously retrograded 15 degrees. Another interesting aspect of this case is the retrogression of the planetary wave which originally was at 150W. NOGAPS handles this phase shift very well.

Within the long wave group the signature of wavenumber 5 persists through 72 hours in both the model and analysis

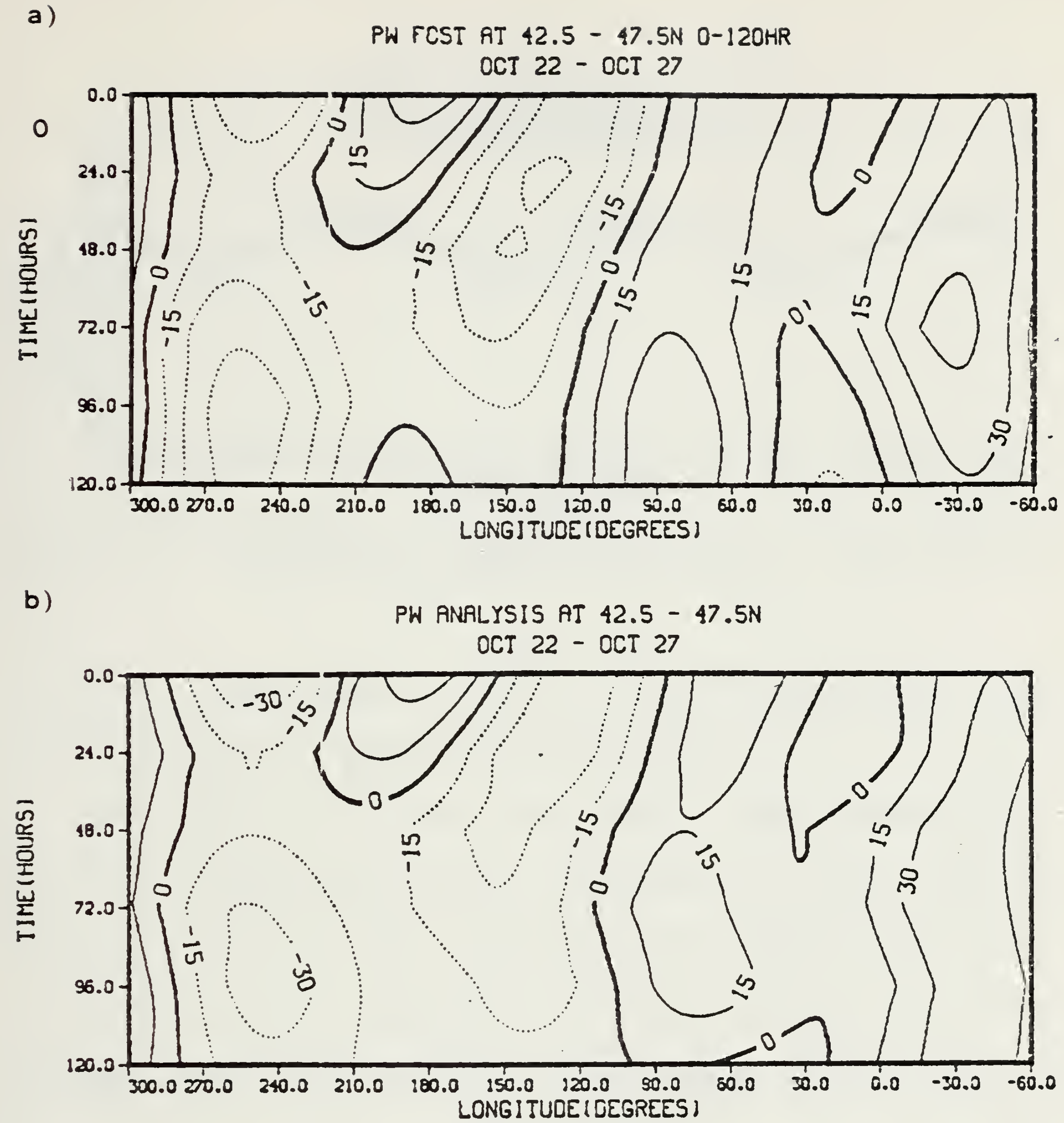

Figure 22. Same as Fig. 8 except for 22-27 Oct

(Figs. 24a and b). A general comparison of observed and forecast long waves shows good agreement on this scale, particularly in phase speeds. The model underforecasts the

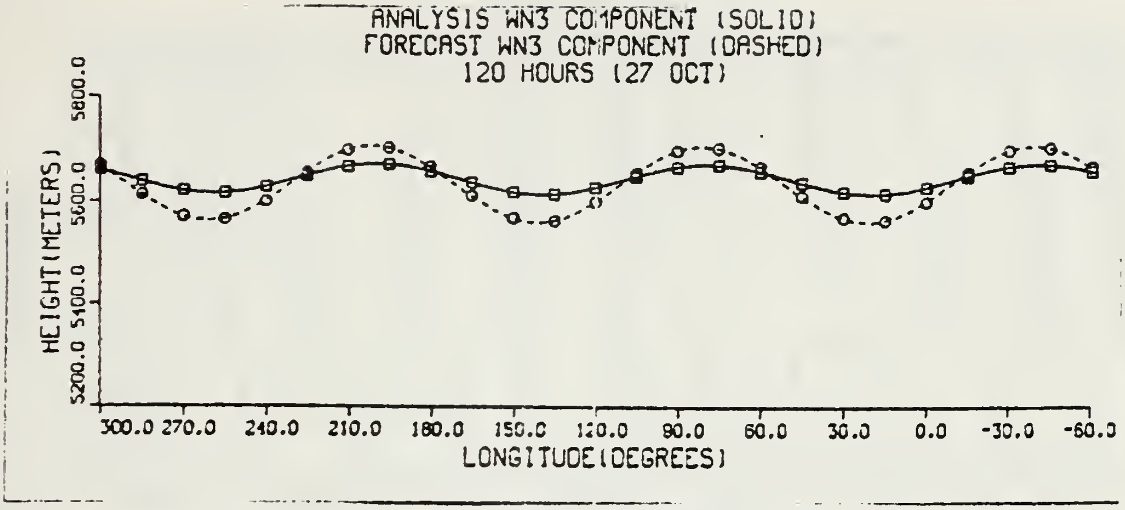

Figure 23. Wavenumber 3 component for Case 3. Same as Fig. 9 except Wavenumber 3 for 27 Oct.

strength of wavenumbers 6 and 7 producing slightly weak amplitudes in the region from 30E to 120E.

However, by 120 hours both observed and forecast patterns show a duel dominance in wavenumbers 5 and 6 with the model amplitude a little too weak in wavenumber 5 and a little too strong in wavenumber 6. In the last 24 hours of the forecast period the atmosphere introduced a sixth trough and ridge by a general retrograding of certain existing features (180W to 40E) by 5 to 10 degrees of longitude. The model introduced a sixth trough and ridge by a rapid eastward movement of certain features (25W to 140E). This incorrect method of handling the dominance shift resulted in phase speed errors in the range of 5 to 15 degrees too fast.

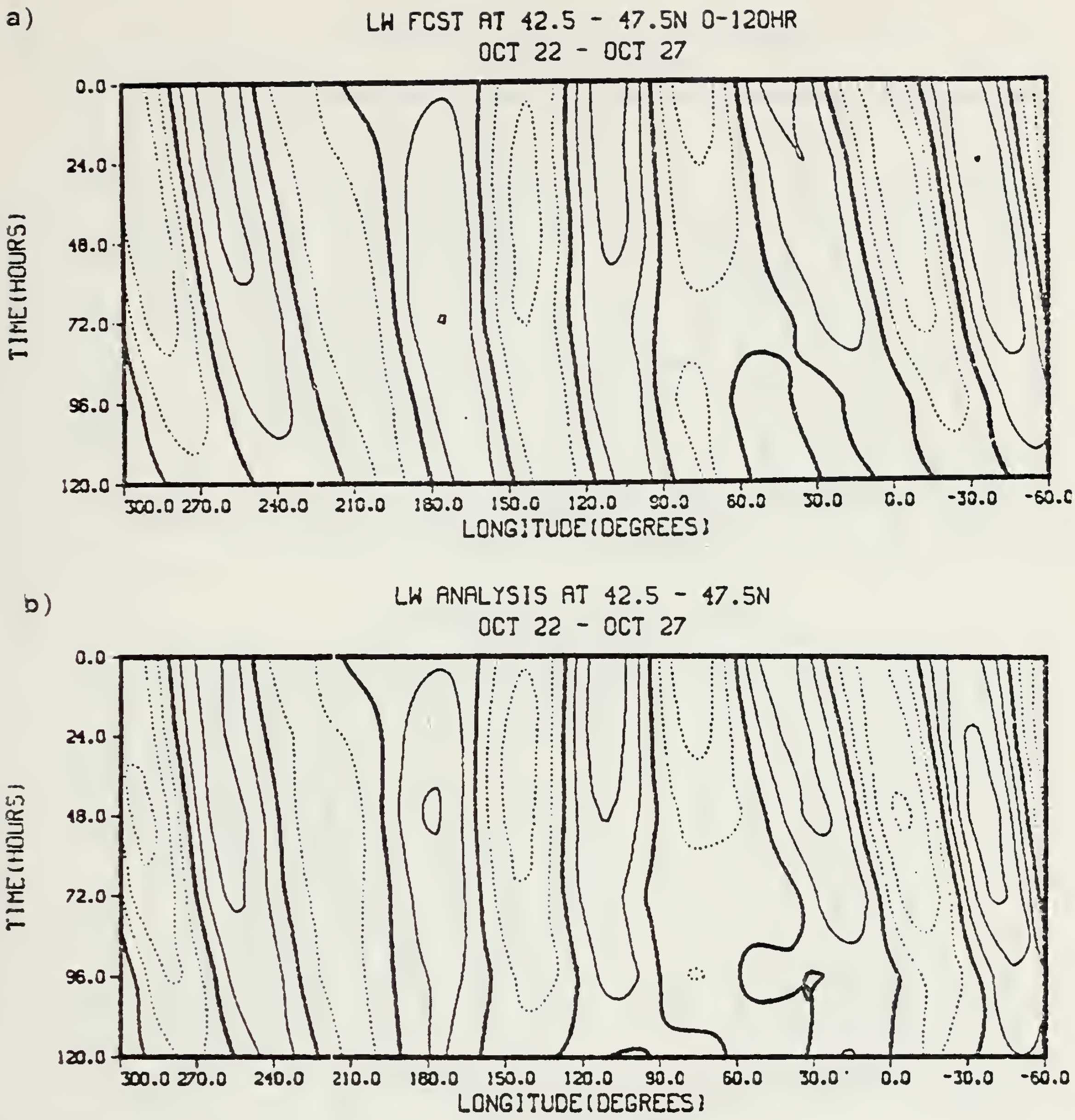

Figure 24. Same as Fig. 10 except for 22-27 Oct

In the medium wave group (Figs. 25a and b) the model correctly began with the signature of wavenumber 9, maintained it through 72 hours then shifted to wavenumber 8

a)

MW FCST FOR 42.5 - 47.5N 0-120H
OCT 22 - OCT 27

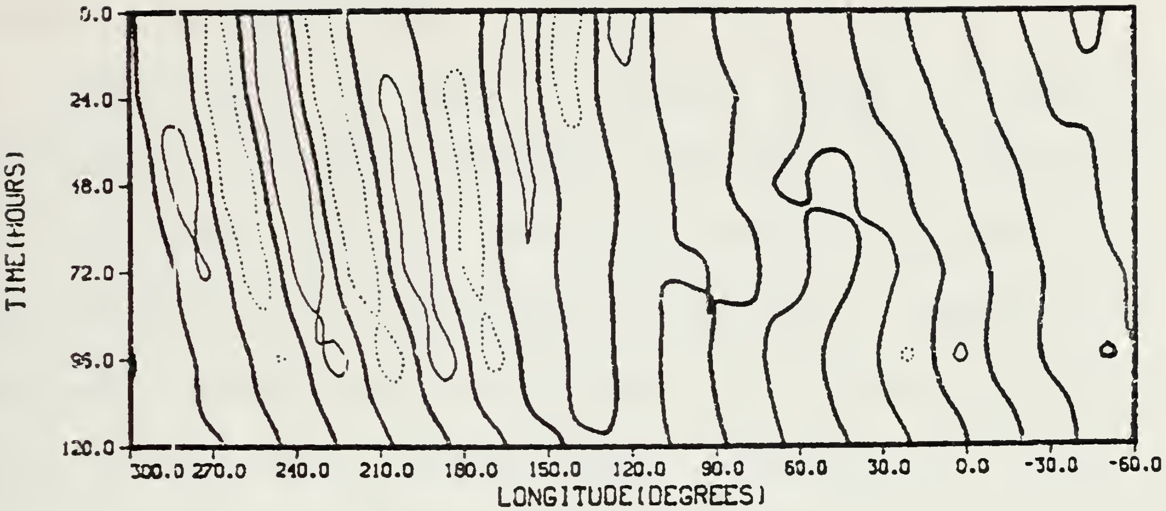

b)

MW ANALYSIS AT 42.5 - 47.5N
OCT 22 - OCT 27

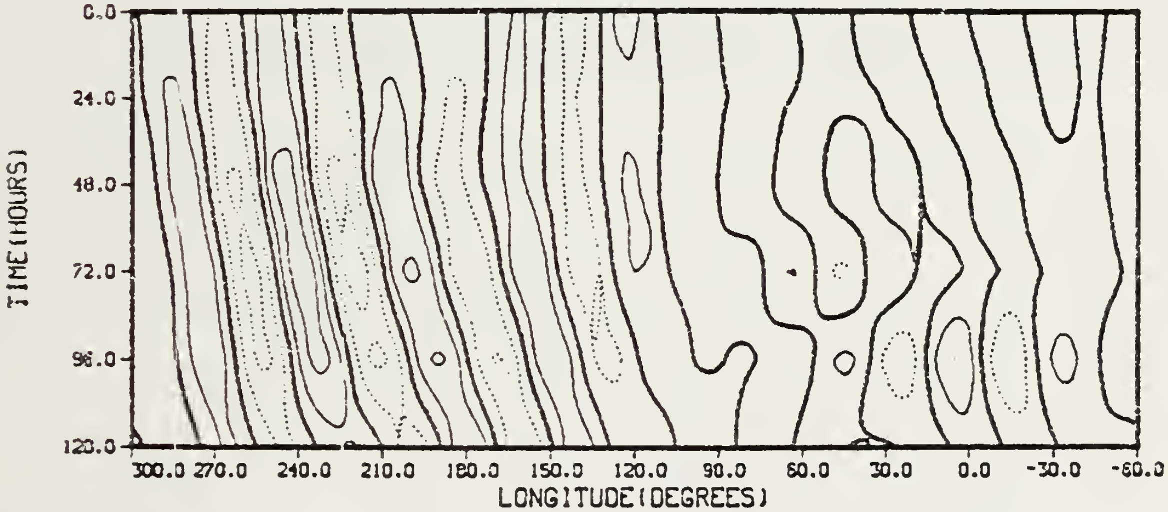

Figure 25. Same as Fig. 11 except for 22-27 Oct

dominance by 120 hours. Both diagrams show their largest amplitudes in the region from 80E to 120W. Overall the model's amplitudes are too weak as a result of consistently

underforecasting the strength of the medium waves. The phase speeds are too fast by approximately 10 degrees in the region from 20E to 160E.

The results of case 3 indicate NOGAPS erroneously shifted the planetary wavenumber dominance into wavenumber 3. The error was large enough to significantly affect the amplitudes of all the wavenumber 3 features. NOGAPS planetary wave phase speed was excellent at 72 hours and still good by 120 hours. The forecast amplitudes of the long waves were only slightly smoothed and long wave phase speeds were excellent at 72 hours but too fast by 120 hours. The medium wave amplitudes were smoothed and phase speeds were too fast.

V. CONCLUSIONS AND SUGGESTIONS FOR FUTURE RESEARCH

In this study one three-day and two five-day NOGAPS 500mb forecasts were spectrally verified. The cases were chosen to reflect three different planetary and long wave situations. In Case 1 the 500mb pattern is characterized by a vigorous three wave pattern. In Case 2 a formation of a blocking high and a shift to a low index flow dominate the 500mb pattern while Case 3 describes the breakdown of a block and a shift to a high index flow.

Two analysis techniques were used to study the observed and forecast spectral statistics. The amplitudes of each wavenumber in the analysis and the forecast are compared at key periods during the forecast and Hovmoller diagrams are prepared for key wavenumber groupings following Baumhefner and Downey (1978). Wavenumber components were grouped into planetary (waves 1-3) long (waves 5-7) and medium waves (waves 8-12) and displayed on trough-ridge diagrams.

In all three cases the most serious errors were concentrated in the planetary waves. The model consistently

failed to correctly predict large amplitude changes in the individual planetary wavenumber components. NOGAPS both predicted large amplitude changes which did not occur in the observations and failed to predict large amplitude changes which did occur in the analysis. In Case 1 the model forecast an erroneously large amplitude increase in wavenumber 1 while in Case 2 NOGAPS smoothed the wavenumber 2 amplitude which had increased dramatically in the analysis. Based on these three cases a systematic error can not be established. The erroneous amplitude shifts caused differences in the wavenumber signatures and made estimates of phase speed errors difficult. Where direct comparisons could be made, planetary wave phase speeds were accurately forecast.

The long wave group (waves 5-7) was the most accurately forecast by NOGAPS. Overall amplitude and phase speed characteristics were well predicted although amplitudes were slightly smoothed by the model and phase speeds tended to be slightly too fast in the regions of increased long wave activity such as in Case 2. In other regions of both slow and fast movement the model showed a high degree of phase speed accuracy.

The medium waves (8-12) verification exhibited some systematic errors. NOGAPS tended to smooth the amplitudes of the medium waves to the point where key features were often lost. Also phase speeds of the medium waves were generally too fast in the model. Specifically, examples of fast phase speeds in Case 1 are in the region from 0E to 120E, in Case 2 from 180W to 30W and in Case 3 from 20E to 160E.

Several suggestions for future research follow from this study. First, the number of forecasts spectrally verified should be increased. Now that the spectral verification software has been prepared, the verification could be done routinely. The goal of the increased number of cases would be to document systematic spectral errors in NOGAPS.

A second area that should be investigated is the relationship between the strength of the circumpolar vortex and the forecast phase speed errors. Variations in the wavenumber zero component can be found by comparing gradients of the mean height of the forecast to the observation. The strength of the circumpolar vortex may be a factor in the phase speeds of the shorter synoptic waves.

A third suggestion involves the question of the optimum north-south interval for verification. This study used eight degrees of latitude for Case 1 and five degrees for Cases 2 and 3. Further studies should examine the effects of narrower or wider latitude bands in the analysis. Similarly the effects of latitude variations on wavenumbers could be determined by using data from different latitudes (60N, 30N, etc).

This study illustrated the utility of diagnostic verification techniques for study of operational numerical prediction models. Future improvement in NOGAPS forecast skill, particularly in the medium range, is dependent in part on the continuing study of the model to isolate its strength and weaknesses.

LIST OF REFERENCES

Arakawa, A. and V.R. Lamb, 1977: Computational design of the basic dynamical processes of the UCLA general circulation model, *Methods in Computational Physics*, *Vol 17*, Academic Press Inc., New York.

Arakawa, A. and W.H. Schubert, 1974: Interaction of a cumulus cloud ensemble with the large-scale environment, Part 1., *J. Atmos. Sci.*, *31*, 647-701.

Barker, E.H., 1981: Analysis and initialization procedure for the Naval Operational Global Atmospheric Prediction System, Report in preparation.

Barnes, S.L., 1964: A technique for maximizing the details in numerical weather map analysis, *J. Appl. Meteor.* *3*, 396-409.

Baumhefner, D. and P. Downey, 1978: Forecasts intercomparisons from three numerical weather prediction models, *Bull. Amer. Meteor. Soc.*, 1245-1279.

Bettge, T.W., 1981: An examination of the characteristics of planetary scale systematic forecast errors, *Preprints of Fifth Conference on Numerical Weather Prediction*, 109-114.

Cullen, M.J.P., S.J. Foreman, J.W. Prince, A.M. Radford and D.R. Roskilly, 1980: Forecast intercomparisons of three numerical weather prediction models from the UK Meteorological Office, *Mon. Wea. Rev.*, *109*, 422-459.

Deardorff, J.W., 1972: Parameterization of the planetary boundary layer for use in general circulation models, *Mon. Wea. Rev.*, *100*, 93-106.

Katayama, A., 1972: A simplified scheme for computing radiative transfer in the troposphere, Technical Report No. 6, Dept. of Meteorology, UCLA.

Lambert, S.J. and P.E. Merilees, 1978: A study of planetary wave errors in a spectral numerical weather prediction model, *Atmosphere-Ocean*, *16*, 197-211.

Lord, S.J., 1978: Development and observational verification of a cumulus cloud parameterization, Ph.D. Thesis, Dept. of Atmos. Sci., UCLA.

Miyakoda, K., G.D. Hembree, R.F. Strickler and I. Shulman, 1972: Cumulative results of extended forecast experiments. I. Model performance for winter cases, *Mon. Wea. Rev.*, *100*, 836-855.

Rosmond, T.E., 1981: NOGAPS: Naval Operational Global Atmospheric Prediction System. *Preprints of Fifth Conference on Numerical Weather Prediction*, 74-79.

Schlesinger, M.E., 1976: A numerical simulation of the general circulation of atmospheric ozone, Ph.D. Thesis, Dept. of Atmos. Sci., UCLA.

Somerville, R., 1980: Tropical influences on the predictability of ultralong waves, *J. Atmos. Sci.*, *37*, 1141-1156.

INITIAL DISTRIBUTION LIST

		No. Copies
1.	Professor Carlyle H. Wash, Code63Cw Department of Meteorology Naval Postgraduate School Monterey, CA 93940	5
2.	Professor Roger T. Williams, Code 63Wu Department of Meteorology Naval Postgraduate School Monterey, CA 93940	1
3.	Professor Robert J. Renard, Code 63Rd Department of Meteorology Naval Postgraduate School Monterey, CA 93940	1
4.	Capt. Peter A Morse Det 4, 3rd Weather Squadron Holloman AFB, NM 88330	3
5.	Capt. Alan R. Shaffer, Code 63 Department of Meteorology Naval Postgraduate School Monterey, CA 93940	1
6.	Professor Christopher N. K. Mooers, Code 68Mr Department of Oceanography Naval Postgraduate School Monterey, CA 93940	1
7.	Library, Code 0142 Naval Postgraduate School Monterey, CA 93940	2
8.	Commander Air Weather Service Scott Air Force Base, IL 62225	1
9.	Air Weather Service Technical Library Scott Air Force Base, IL 62225	1
10.	Commander Air Force Global Weather Central Offutt Air Force Base, NE 68113	1
11.	Capt. Brian Van Orman Program Manager, AFIT/CIRF Air Force Institute of Technology Wright-Patterson Air Force Base, OH 45433	1

12. Commanding Officer 1
Fleet Numerical Oceanography Center
Monterey, CA 93940

13. Commanding Officer 1
Naval Environmental Prediction Research Facility
Monterey, CA 93940

14. Commander (Air-370) 1
Naval Air Systems Command
Headquarters
Department of the Navy
Washington, D. C. 20361

15. Defense Technical Information Center 2
Cameron Station
Alexandria, VA 22314

16. Director 1
Naval Oceanography Division
Naval Observatory
34th and Massachusetts Avenue NW
Washington, D.C. 20390

17. Commanding Officer 1
Naval Oceanographic Office
NSTL Station
Bay St. Louis, MS 39522

18. Office of Naval Research (Code 480) 1
Naval Ocean Research and Development Activity
NSTL Station
Bay ST. Louis, MS 39522

19. Chairman, Oceanography Department 1
U. S. Naval Academy
Annapolis, MD 21402

20. Chief of Naval Research 1
800 N. Quincy Street
Arlington, VA 22217

Thesis 200414
M83975 Morse
c.1
NOGAPS verification using spectral components.

200414
Thesis
M83975 Morse
c.1
NOGAPS verification using spectral components.

thesM83975
NOGAPS verification using spectral compo
3 2768 001 91735 4
DUDLEY KNOX LIBRARY